

REPORT DOCUMENTATION PAGE		READ INSTRUCTIONS BEFORE COMPLETING FORM
1. REPORT NUMBER TR 7193	2. GOVT ACCESSION NO.	3. RECIPIENT'S CATALOG NUMBER
4. TITLE (and Subtitle) TRANSIENT RESPONSE OF MULTIDIMENSIONAL ARRAYS		5. TYPE OF REPORT & PERIOD COVERED
		6. PERFORMING ORG. REPORT NUMBER
7. AUTHOR(s) Paul D. Koenigs		8. CONTRACT OR GRANT NUMBER(s)
9. PERFORMING ORGANIZATION NAME AND ADDRESS New London Laboratory Naval Underwater Systems Center New London, Connecticut 06320		10. PROGRAM ELEMENT, PROJECT, TASK AREA & WORK UNIT NUMBERS A70215 61152N ZR0000101
11. CONTROLLING OFFICE NAME AND ADDRESS		12. REPORT DATE 26 June 1984
		13. NUMBER OF PAGES
14. MONITORING AGENCY NAME & ADDRESS (if different from Controlling Office)		15. SECURITY CLASS. (of this report) UNCLASSIFIED
		15a. DECLASSIFICATION/DOWNGRADING SCHEDULE
16. DISTRIBUTION STATEMENT (of this Report) Approved for public release; distribution unlimited.		
17. DISTRIBUTION STATEMENT (of the abstract entered in Block 20, if different from Report)		
18. SUPPLEMENTARY NOTES		
19. KEY WORDS (Continue on reverse side if necessary and identify by block number) Conformal arrays Imaging Near field response Continuous arrays Impulse response Scanned arrays Distributed arrays Line arrays Steady state Focused arrays Localization Transient		
20. ABSTRACT (Continue on reverse side if necessary and identify by block number) The transient pressure field generated by baffled pistons has received considerable attention because of its fundamental importance in the analysis of many acoustical problems. Although considerable work has been devoted to the analysis of the steady state response of line arrays, little effort has been devoted to develop a systematic approach to investigate their transient behavior. A simple approach to evaluate the transient and steady response of		

20. (Cont'd)

transmitting and receiving arrays is developed in this thesis. This method is an extension of Stepanishen's spatial impulse response technique to free field line arrays of finite elements with time delay beamformers. An impulse response function is defined at a field point resulting from a distribution of sources and arbitrary time delays. The transient pressure field arising from the element distribution and time delay is then obtained by convolving the time derivative of the impulse response with the excitation waveform.

The impulse response for several discrete element line array systems is obtained and shown to be a series of impulses. The strength and location of the impulses is related to the geometrical properties of the array, the beamformer time delays and the field point.

The impulse response for a continuous line array with an internal propagation speed is developed as a linear superposition of three dimensional point sources with initial excitation times dependent on their location within the array. In this instance the magnitude and duration of the impulse response is dependent on the geometrical properties of the array, the speed of propagation within the array and media, and the location of the field point. The receiving response of an array can also be evaluated using the same impulse response technique.

Based on the numerical results obtained and favorable comparisons with other techniques when possible, it appears the impulse response technique is a viable approach for analyzing the formidable problem posed by array systems which generate or receive transient pressure fields. The technique yields a spatial impulse response which is dependent on element size, array geometry and the beamformer. The impulse response can then be convolved with a variety of excitation waveforms to conduct an array system analysis as a function of waveform design or received signal.

NUSC Technical Report 7193
26 June 1984

LIBRARY
RESEARCH REPORTS DIVISION
NAVAL POSTGRADUATE SCHOOL
MONTEREY, CALIFORNIA 93943

Transient Response of Multidimensional Arrays

Paul D. Koenigs
Surface Ship Sonar Department



Naval Underwater Systems Center
Newport, Rhode Island / New London, Connecticut

Preface

The material contained in this report was prepared in partial fulfillment of the requirements for the degree of Master of Science in Ocean Engineering at the University of Rhode Island. This technical report was prepared under NUSC Project No. A70215, "Transient Response of Multidimensional Arrays," Principal Investigator, Paul D. Koenigs; sponsored by the NUSC in-house Independent Research program under Program Element 61152N, Navy Subproject No. ZR0000101, Mr. Gary Morton, Program Manager, Director of Navy Laboratories.

Acknowledgments

I wish to express my gratitude to Professor Peter R. Stepanishen, my advisor and motivating force for this study. Without his guidance and perception many of the difficulties encountered in this study would not have been overcome.

I am greatly appreciative of the Office of Naval Research which provided the funds necessary to undertake this study and the Naval Underwater Systems Center which provided many of the clerical and computational facilities utilized in completing this thesis.

I would also like to thank my supervisor at NUSC, Mr. W. R. Schumacher, for his encouragement and flexibility which made this task markedly easier.

Reviewed and Approved: 26 June 1984



W. A. Von Winkle
Associate Technical Director for Technology

The author of this report is located at the
New London Laboratory, Naval Underwater Systems Center,
New London, Connecticut 06320

TABLE OF CONTENTS

Page

LIST OF FIGURES	iii
CHAPTER I. INTRODUCTION.	1
CHAPTER II. THEORY	4
A. Introduction.	4
B. Linear System Concepts and Signal Processing.	4
C. Impulse Response Method	8
D. Beamforming	11
E. Impulse Response of Pulse-Echo System	14
CHAPTER III. SELECTED RESULTS.	18
A. Introduction.	18
B. Simple Source	18
C. Line Array of Simple Sources.	21
D. Continuous Line Source.	26
E. Frequency Focused and Scanned Line Array.	34

TABLE OF CONTENTS (cont.)

	<u>Page</u>
CHAPTER IV. NUMERICAL RESULTS.	42
A. Introduction.	42
B. Continuous Line Array	42
C. Discrete Line Array	50
1. Colinear Array of Discrete Elements.	50
2. Curved Array of Discrete Elements.	55
3. Frequency Focused and Scanned Line Array	63
CHAPTER V. SUMMARY AND CONCLUSIONS	81
LITERATURE CITED.	84
SELECTED BIBLIOGRAPHY	85

- Figure 2-1. Coordinate Definition.
- Figure 2-2. Conceptual Array and Beamformer.
- Figure 2-3. Pulse Echo System Block Diagram.
- Figure 3-1. Impulse Response of Simple Source.
- Figure 3-2. Velocity Potential and Pressure Resulting from CW, LFM and Boxcar Source Strength Functions.
- Figure 3-3. Line Array of Simple Sources and Corresponding Impulse Response.
- Figure 3-4. Dependence of Transient Array Response on Frequency.
- Figure 3-5. Impulse Response of Continuous Line Source.
- Figure 3-6. Farfield Geometry for Continuous Line Source.
- Figure 3-7. Impulse Response of Continuous Line Source as Function of n .
- Figure 3-8. Conceptual Diagram of Frequency Focused and Scanned Line Array.
- Figure 3-9. Instantaneous Frequency of LFM Chirp.
- Figure 3-10. Reciprocal Scanning Geometries for a Pulsed Array.
- Figure 4-1. Continuous Line Array.
- Figure 4-2. Impulse Response of Continuous Line Source with Internal Propagation Speed
- Figure 4-3. Transient Pressure Response of a Continuous Line Array.
- Figure 4-4. Spatial Sampling Points for Continuous Line Array.
- Figure 4-5. Transient Pressure Response for Three Ranges of n .
- Figure 4-6. Time Derivative of Impulse Responses for Five Element Array With and Without Beamforming.
- Figure 4-7. Conceptual Diagram of Thirty-Five Element Colinear Line Array and Beamformer.
- Figure 4-8. Time Derivative of Colinear Array Impulse Response for Four Field Points.

- Figure 4-9. Transient Pressure Response of Colinear Array for Four Field Points.
- Figure 4-10. Conceptual Diagram of Thirty-Five Element Curved Line Array and Beamformer.
- Figure 4-11. Time Derivative of Curved Array Impulse Response for Four Field Points along the Line $y = 9$ cm.
- Figure 4-12. Transient Pressure Response of Curved Array for Four Field Points along the Line $y = 9$ cm.
- Figure 4-13. Time Derivative of Curved Array Impulse Response for Four Field Points along the line $x = 3$ cm.
- Figure 4-14. Transient Pressure Response of Curved Array for Four Points along the Line $x = 3$ cm.
- Figure 4-15. Pressure Time Series from Scanned and Focused Array in the Farfield.
- Figure 4-16. Initial Disturbance Time at a Field Point versus Element Position along $y = 10$ cm Line.
- Figure 4-17. Impulse Response for Scanned and Focused Array.
- Figure 4-18. Instantaneous Frequency as Function of Element Location Required for Focusing at One Location.
- Figure 4-19. Transient Response from a Scanned and Focused Array Using the Impulse Response Technique.
- Figure 4-20. Transient Response with Interelement Spacing (1.3 mm).
- Figure 4-21. Signal Response from Individual Elements and Array at a Focal Point.
- Figure 4-22. Transient Response from a Scanned and Focused Array of Extended Elements.
- Figure 4-23. Conceptual Diagram of Frequency Focused and Scanned Transmitting Array and Time Delay Beamforming Receiving Array.
- Figure 4-24. Transient Response of Receiving Array Focused on a Target.
- Figure 4-25. Transient Response of Receiving Array as Function of Receiver Beamformer.

I. INTRODUCTION

The radiated field generated by baffled pistons has necessarily received considerable attention because of its fundamental importance in the analysis of many acoustical systems. Although the field produced by a piston of arbitrary shape is widely studied, most efforts can be traced to a few fundamental methods of analysis (Harris). Each approach can be derived from the wave equation with boundary and initial conditions.

The first studies of the baffled piston made use of the Rayleigh surface integral solution for the time dependent velocity potential. The Rayleigh integral is a mathematical statement of Huygen's principle. This principle states that every point on a vibrating surface may be considered a source of outgoing spherical waves and the net field can be obtained using linear superposition.

The other two methods can be derived from the Rayleigh integral in a very similar manner. In each approach the surface integral is transformed into a line integral expression by means of a translation of the coordinate system. The order in which the integration is performed determines whether the Schock or convolution approach will be obtained.

The Schock integral decomposes the transient field into geometrical and diffraction waves (Harris, *ibid*). The convolution integral method introduces a spatial impulse response and the field for any arbitrary source motion can be obtained using the fundamental concepts of linear system theory.

Apparently Morse was the first to derive an expression for the transient field arising from a circular piston but Stepanishen is the best known author of articles related to the convolution integral representation. His development is based on a Green's function solution to the wave equation. The radiated field is expressed in terms of a convolution integral which lends itself to the study of other interesting transient field problems.

Although considerable work has been devoted to the analysis of the steady state response of line arrays, little effort has been devoted to a systematic analysis of the transient response of these arrays. The subject of this thesis is the extension of Stepanishen's (Stepanishen, Phd. Thesis) impulse response technique to free field line arrays of finite elements with time delay beamformers. A simple approach to evaluate the transient and steady state response of transmitting and receiving arrays is developed and used to obtain numerical results.

The present development is based on a Green's function solution to the time dependent wave equation. An impulse response function is defined at a spatial point resulting from a distribution of sources and arbitrary time delays. The transient pressure field arising from the source distribution and time delays is then obtained by convolving the time derivative of a source function with the impulse response.

The development of the impulse response technique as extended to include point source distributions and beamformers is presented in Chapter II. The development is then expanded in a straightforward manner to include a complete pulse-echo system.

The impulse response technique is then used in Chapter III to evaluate the impulse response and transient pressure field for several

cases where the results can be obtained in closed form or via other methods. These cases serve to illustrate, clarify, validate and demonstrate the utility of the impulse response technique.

In Chapter IV the numerical results for several complex systems, comprised of simple or finite size sources, such as curved arrays and frequency focused and scanned line arrays are presented and analyzed. Through these examples the usefulness and applicability of the method will become apparent.

Chapter V contains a summary of the conclusion reached in this thesis and touches briefly on several areas where the technique can be expanded to systems more complex than those examined in this thesis.

II. THEORY

A. Introduction

In this chapter, the salient linear system concepts and signal processing requirements needed in the formulation and computer implementation of the transient array response problem are presented. A brief discussion of the basic theory required to describe the impulse response of arrays and beamformers is followed by a discussion of the impulse response of a pulse-echo system.

B. Linear System Concepts and Signal Processing

A system in this study is meant to imply devices which process or modify signals. A device, in general, will perform some type of operation (for example, a mathematical identity or a digital computer algorithm) necessary to synthesize more complex problems. An intent of this study, as mentioned earlier, is to perform an analysis of the transient response of multidimensional arrays. Within this context a system analysis is to study the output of a system as a function of various input signals and system parameters. A signal represents some physical quantity such as voltage, pressure or velocity.

Three special signal types require definition before proceeding. The impulse function, denoted by $\delta(t)$, is a signal of unit area which vanishes everywhere except where the functional argument is zero. It follows then that a time shifted delta function satisfies the following identity (Papuolis)

$$\int_{-\infty}^{+\infty} \phi(T) \delta(t_0 - T) dT = \phi(t_0) \quad (2.1)$$

The unit step function is defined as:

$$\begin{aligned} u(t) &= 0 & ; & \quad t < 0 \\ &= 1 & ; & \quad t \geq 0 \end{aligned} \quad (2.2)$$

Based on the unit step function it is convenient to define a rectangular or boxcar function as:

$$\begin{aligned} b(t) = u(t - t_1) - u(t - t_2) &= 0 & ; & \quad t < t_1 \\ &= 1 & ; & \quad t_1 \leq t \leq t_2 \\ &= 0 & ; & \quad t > t_2 \end{aligned} \quad (2.3)$$

In many cases it is desirable to express the output of a system in terms of an input and the impulse response. By definition, the impulse response, $h(t)$, is the output of a linear, time invariant system when the input is a delta function. This leads to the familiar convolution integral:

$$y(t) = \int_0^t x(T) h(t - T) dT \quad (2.4)$$

which relates the output $y(t)$ to the input signal $x(t)$ and the impulse response of the system. This equation will also be written as:

$$y(t) = x(t) * h(t) \quad (2.5)$$

where the asterisk denotes the convolution process.

If the Fourier transform of $f(t)$ is defined as

$$F(\omega) = \int_{-\infty}^{+\infty} f(t) e^{-j\omega t} dt \quad (2.6)$$

then a transform pair can be expressed as:

$$f(t) \Leftrightarrow F(\omega) \quad (2.7)$$

where

$$f(t) = \frac{1}{2\pi} \int_{-\infty}^{+\infty} F(\omega) e^{j\omega t} d\omega. \quad (2.8)$$

The evaluation of the convolution in Eq. 2.5 can then be accomplished in the frequency domain using the following equation

$$y(t) = F^{-1} \{Y(\omega)\} = F^{-1} \{X(\omega) H(\omega)\} \quad (2.9)$$

where capital letters indicate a transform and F^{-1} denotes the inverse Fourier transform operator. It is noted that the Fourier transform of the output of a linear system is given by the product of the system transfer function and the Fourier transform of the input signal (Brigham).

To analyze complex systems using digital computers, it is necessary to develop discrete forms of the system functions. The notation $f[n]$ will mean an array of numbers defined for every integer n . This sequence of numbers is the discrete form of an incrementally sampled continuous function. For example, given a function $f(t)$ the sequence

$$f[n] = f(nT) \quad (2.10)$$

obtained by samplings $f(t)$ in increments of T is a discrete form of the function.

A general discrete form for the output of a linear system $y[n]$ to an arbitrary input $x[n]$ using a sampled version of the impulse response $h[n]$ can be expressed as:

$$y[n] = \sum_{k=-\infty}^{\infty} x[k] h[n-k] = x[n] * h[n] \quad (2.11)$$

For the case when the impulse response is casual and $x[k] = 0$ for $k < 0$, the lower limit is 0 and the upper limit is N .

A discrete Fourier transform pair may be defined as follows:

$$f(nT) = \frac{1}{N} \sum_{m=0}^{N-1} F\left(\frac{m}{NT}\right) e^{-j2\pi \frac{mn}{N}} ; \quad m = 0, 1, \dots, N-1 \quad (2.12)$$

$$F\left(\frac{m}{NT}\right) = \sum_{n=0}^{N-1} f(nT) e^{-j2\pi \frac{mn}{N}} ; \quad n = 0, 1, \dots, N-1 \quad (2.13)$$

This requires both the time and frequency domain functions to be periodic.

The preceding expressions relate N samples of time and N samples of frequency and approximates the continuous Fourier transform pair of Eq. (2.7). The validity of this approximation is dependent on the frequency and time extent of the function $f(t)$.

This study addresses, to a large extent, transient phenomena which infers finite duration waveforms. Because the signals and the impulse response function used in this study are time limited, sampling will result in aliasing. It will therefore be necessary to choose sampling intervals such that aliasing of either the impulse or signal transform is reduced to an acceptable level.

C. Impulse Response Method

Consider the problem of determining the time dependent pressure at a spatial point r resulting from a specified spatial and temporal velocity distribution of an array of sources in an ideal fluid of density ρ and acoustic propagation speed c . The inhomogeneous wave equation, formulated in terms of a velocity potential ϕ and source terms Q is

$$\nabla^2 \phi - \frac{1}{c^2} \frac{\partial^2 \phi}{\partial t^2} = -Q \quad (2.14)$$

Using a Green's function approach (Morse and Ingard) the solution to this equation for unbounded medium is (see figure 2.1 for coordinate definitions)

$$\phi(\vec{r}, t) = \int_0^t dt_0 \int_{R_3} d\vec{r}_0 g(\vec{r}, t | \vec{r}_0, t_0) q(\vec{r}_0, t_0) \quad (2.15)$$

where the time dependent Green's function is

$$g(\vec{r}, t | \vec{r}_0, t_0) = \frac{\delta(t - t_0 - \frac{|\vec{R}|}{c})}{4\pi |\vec{R}|} \quad (2.16)$$

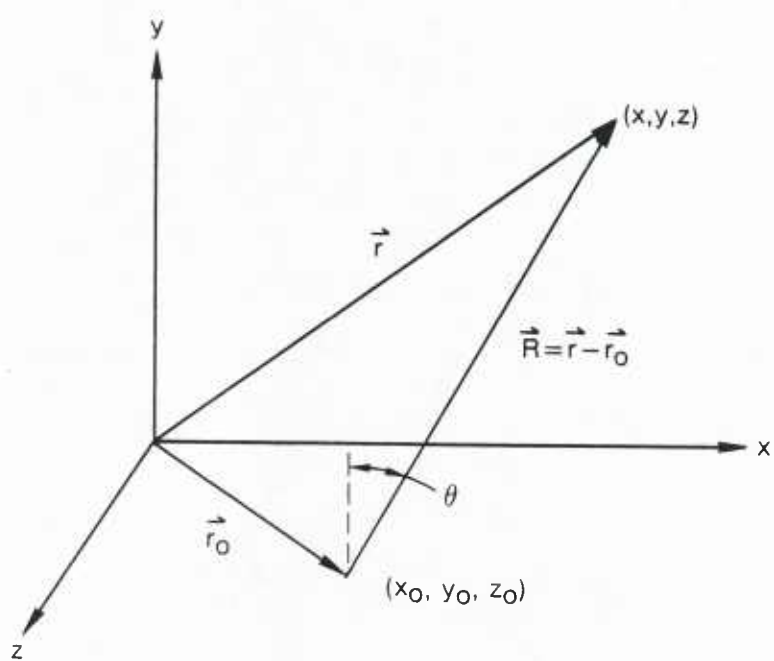


Figure 2-1. Coordinate Definition.

The pressure may then be obtained from

$$p(\vec{r}, t) = \rho \frac{\partial \phi(\vec{r}, t)}{\partial t} \quad (2.17)$$

When the time dependence of the source term is independent of its spatial coordinates and is expressed in terms of a source strength $q(t)$, Eq. (2.15) may be written as

$$\phi(\vec{r}, t) = \int_0^t q(t_0) dt_0 \int_{R_3} \frac{\delta(t - t_0 - \frac{|\vec{R}|}{c})}{4\pi |\vec{R}|} d\vec{r}_0 \quad (2.18)$$

where R_3 denotes the spatial domain of the source. Defining an impulse response at the spatial point of interest resulting from a distributed source excited at t_0 as

$$h(\vec{r}, t) = \int_{R_3} \frac{\delta(t - t_0 - \frac{|\vec{R}|}{c})}{4\pi |\vec{R}|} d\vec{r}_0 \quad (2.19)$$

and substituting into Eq. (2.18) we obtain a convolution integral for $\phi(\vec{r}, t)$ of:

$$\phi(\vec{r}, t) = q(t) * h(\vec{r}, t) \quad (2.20)$$

When the distributed source or array is composed of N simple sources, the source strength can be expressed as

$$q(\vec{r}, t) = \sum_{n=1}^N q(t - t_n) \delta(\vec{r} - \vec{r}_n) \quad (2.21)$$

where \vec{r}_n denotes the source locations and t_n is the time at which the n th source is excited. For this case $\phi(\vec{r}, t)$ can be expressed in the form of Eq. (2.20) where the spatial integral in Eq. (2.19) can be written as

$$h(\vec{r}, t) = \sum_{n=1}^N \frac{\delta(t - t_n - \frac{|\vec{r} - \vec{r}_n|}{c})}{4\pi |\vec{r} - \vec{r}_n|} \quad (2.22)$$

Equation 2.22 represents the impulse response at a spatial point \vec{r} arising from a collection of sources located at points \vec{r}_n and initially excited at some time t_n .

D. Beamforming

An array problem in general consists of summing the outputs of individual elements. A beamformer in general is a device which rearranges the element outputs such that an overall increase in some performance parameter is noted. For a monochromatic input signal the response of a simple beamformer and array, containing N elements at a point r is of the form

$$R(t) = \text{Re} \left\{ \sum_{n=1}^N \frac{A_n}{|\vec{R}_n|} e^{j(\omega t - \vec{k} \cdot \vec{R}_n - \psi_n)} \right\} \quad (2.23)$$

where $k = \omega/c$ and kR_n is the signal phase at a distance R_n and ψ_n may be associated with a preselected phase adjustment. A_n is an arbitrary amplitude shading factor. Making the usual far-field assumptions, factoring out the time dependence, and setting the shading weight to unity, the above equation reduces to the well known beam pattern function of the form $\sin N\psi/\sin\psi$. While this formulation is simple, there are no computational problems with extending Eq. (2.23) to more complex situations such as shading or when wavefront curvature is appreciable. The expression for the proper phase adjustment merely becomes more complex (Steinberg). However, the solution is still only for the monochromatic steady state case.

As shown, the transient response of an array is relatively easy to compute as long as it is possible to determine its impulse response. The basic problem is to develop the impulse response for an array with a beamformer. Note in equation 2.22, t_n is an arbitrary time when the n th element is excited and may be controlled as in a time delay beamformer. Furthermore, $|\vec{R}_n|/c$ is the time required for a disturbance originating at the n th element to reach the field point. This can also be controlled to some extent by adjusting the location of the elements. This is a form of a geometric or spatial beamforming.

Consider for example the array and beamformer depicted in figure 2.2. As shown, t_n represents a time delay for the disturbance $\delta(t)$. The disturbance is then propagated at speed c and arrives at (x,y) at $t = t_n + |\vec{R}_n|/c$. It is easy to see that when

$$t_n + \frac{|\vec{R}_n|}{c} = t_{n+1} + \frac{|\vec{R}_{n+1}|}{c} \quad (2.24)$$

all disturbance arrive at the same time thus maximizing the impulse response function.

Thus it may be stated that equation 2.22 is the correct equation for the impulse response of an array of simple sources with a beamformer where t_n is associated with a temporal beamformer and $|\vec{R}_n|/c$ with a spatial beamformer.

E. Impulse Response of Pulse-Echo System

Thus far the development has concentrated on the spatial impulse response function of an active array and beamformer at the spatial point of interest. To extend this study to include the transient response of a pulse-echo system consider the block diagram of figure 2.3(a).

The system consists of a sending array with components denoted by s and n subscripts and a receiving system denoted by r and m subscripts. Because the time delay beamformers, array elements and media paths for the transmit and receive arrays are linear casual systems connected in cascade, they may be rearranged. By assuming each element in a given array is electrically and mechanically similar and collecting the time delay and media delay systems into one term (see Eq. (2.22)) the diagram can be redrawn in simpler form (figure 2.3(b)) which closely resembles the form illustrated by Stepanishen (Stepanishen, JASA, 1981). In this diagram the transmit element transfer function $G_s(\omega)$ relates the excitation voltage $E_s(\omega)$ to the source strength $Q(\omega)$. The source strength $q(t)$ is the instantaneous media flow away from the source where

$$q(t) \rightleftharpoons Q(\omega) \quad . \quad (2.25)$$

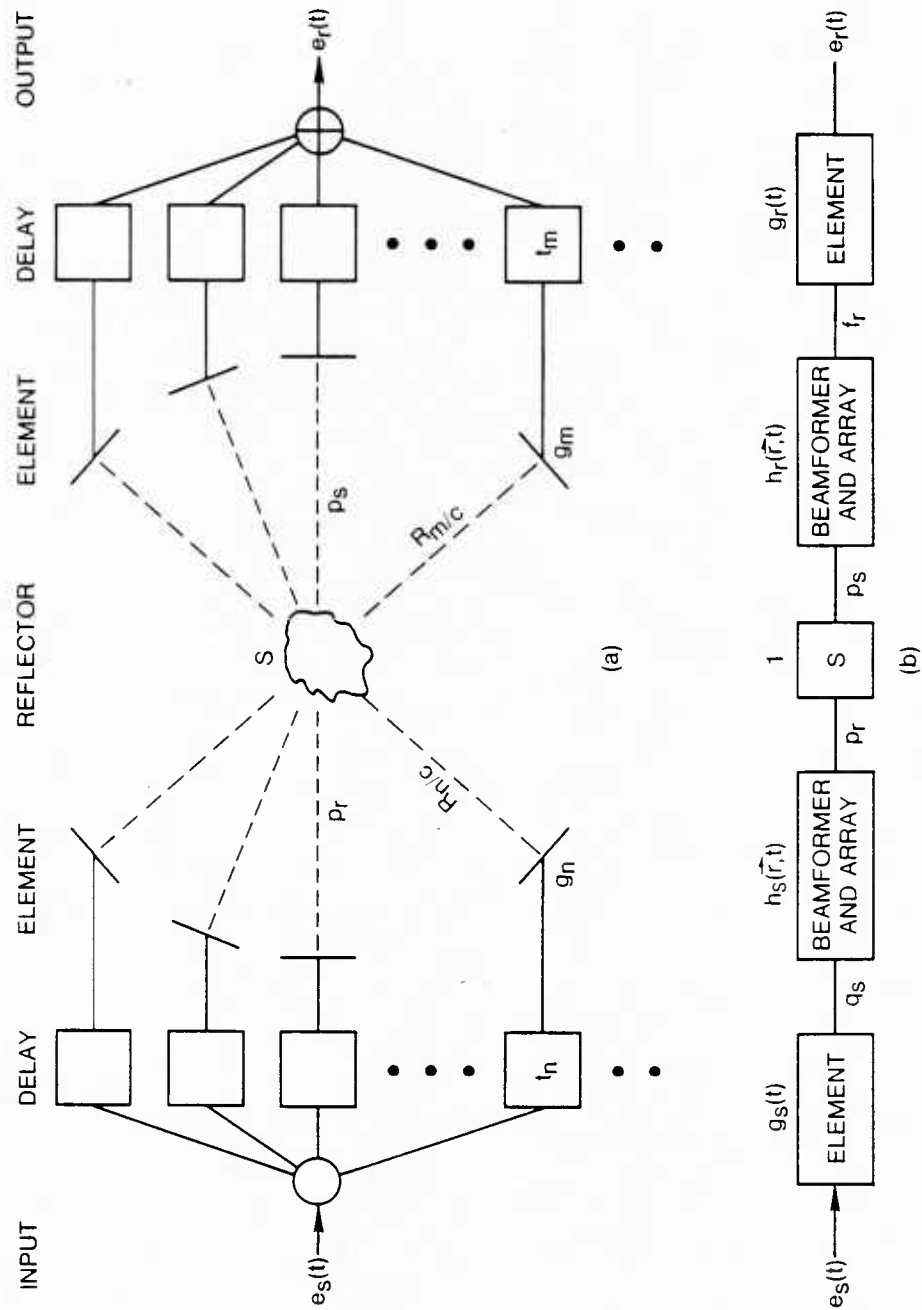


Figure 2-3. Pulse Echo System Block Diagram.

Similarly the receive element transfer function $G_r(\omega)$ relates the force $F_r(\omega)$ on the transducer to the voltage output $E_r(\omega)$.

The total system response may now be formulated using the following equations:

$$q_s = g_s(t) * e_s(t)$$

$$p_s = \rho \frac{\partial}{\partial t} q_s(t) * h_s(\vec{r}, t)$$

let $S = 1$; ideal reflector

$$p_r = p_s$$

$$f_r = p_r(t) * h_r(\vec{r}, t)$$

and finally

$$e_r(t) = \rho \frac{\partial}{\partial t} \left\{ e_s(t) * g_s(t) * h_s(\vec{r}, t) * h_r(\vec{r}, t) * g_r(t) \right\} \quad (2.26)$$

Equation 2.27 describes the transient response of a pulse echo array system containing time delay and spatial beamformers and provides the means to conduct a system analysis. If for example the transmit and receive elemental sources are ideal then $g_s(t) = g_r(t) = K\delta(t)$. If the beamformers are also ideal, then

$$h_s(\vec{r}, t) = N\delta(t - t_s)/4\pi|\vec{R}_s| \quad ; \quad h_r(\vec{r}, t) = N\delta(t_s - t_r)/4\pi|\vec{R}_r|$$

In this case if $e_s(t)$ is a sinusoidal pulse the received voltage output $e_r(t)$ is also a sinusoidal pulse of the same length as the original pulse but is delayed in time an amount $(t_s + t_r)$. If the beamformers are not focused on the ideal target the impulse response decreases in amplitude and exhibits some temporal spread. This results in a decreased output voltage somewhat longer than the original pulse.

III. SELECTED RESULTS

A. Introduction

The general theory of the impulse response approach to examine the transient behavior of the acoustic field arising from an array system as a function of space, time and source function was presented in the preceeding chapter. Since the problem becomes complex very quickly, it is worthwhile to examine a few simple cases for which solutions via other techniques are available for comparative purposes. These cases will serve to illustrate the validity and utility of the impulse response technique and perhaps clarify the approach.

B. Simple Source

The impulse response at a field point resulting from a simple source can be obtained directly from Eq. (2.22) and is shown in figure 3.1. The velocity potential is simply the convolution of an impulse and a source strength function. The pressure may then be calculated using Eq. (2.17). The velocity potential and pressure for three common source strength functions are shown in figure 3.2(a) and (b).

For the case when the source strength term is a monochromatic sinusoidal pulse of period T and amplitude S the pressure is given by

$$p(t) = -\frac{\rho c k}{4\pi r} S \cos(\omega t - kr) ; 0 \leq t - \frac{r}{c} \leq T \quad (3.1)$$

which is the same equation found in Morse and Ingard. For the frequency modulated source function of similar amplitude, period and a slide constant μ the pressure is:

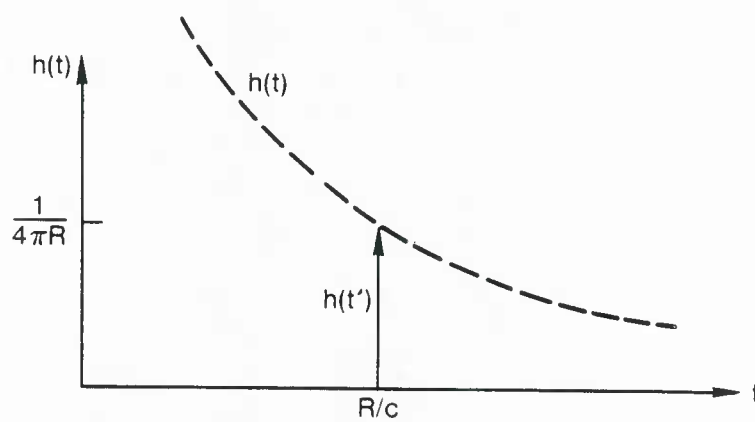


Figure 3-1. Impulse Response of Simple Source.

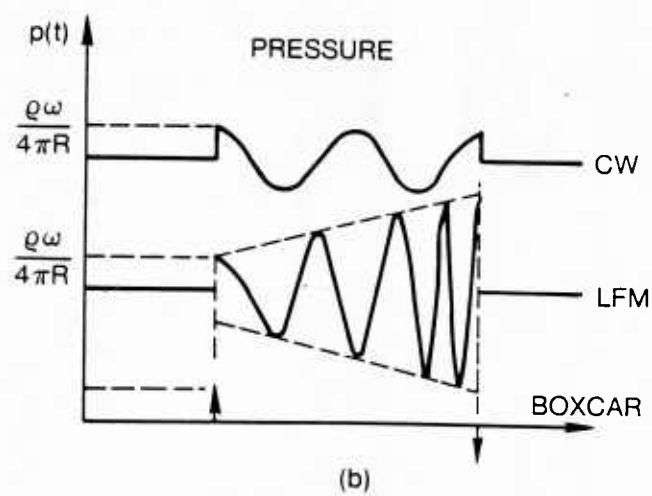
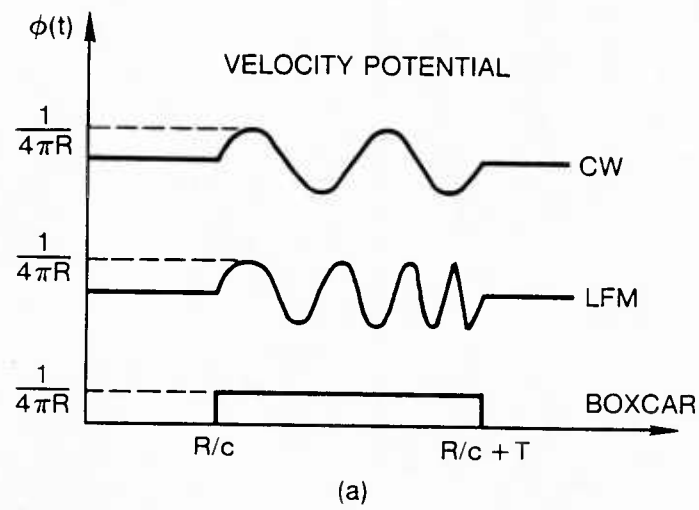


Figure 3-2. Velocity Potential and Pressure Resulting from CW, LFM and Boxcar Source Strength Functions.

$$p(t) = -\frac{\rho}{4\pi r} \left[\omega + u \left(t - \frac{r}{c} \right) \right] \cos \left[\omega t - kr + \frac{u}{2} \left(t - \frac{r}{c} \right)^2 \right] \quad (3.2)$$

where $0 \leq t - r/c \leq T$

Thus, the amplitude of the pressure is linearly dependent on time. In the case of the rectangular source function the pressure is simply two impulse functions of opposite sign as noted on the figure.

C. Line Array of Simple Sources

A straightforward extension of the simple source is a line array consisting of N simple sources located a distance d apart as illustrated in figure 3.3(a). The farfield impulse response when all sources are excited simultaneously, based on Eq. (2.22) is

$$h(\vec{r}, t) = \frac{1}{4\pi r} \sum_{n=1}^N \delta \left(t - \frac{|\vec{R}_n|}{c} \right) \quad (3.3)$$

where

$$|\vec{R}_n| = |\vec{r}| - nd \sin \theta.$$

Note that t_i and t_f where

$$t_i = \frac{r}{c} - \frac{Nd \sin \theta}{c}$$

$$t_f = \frac{r}{c}$$

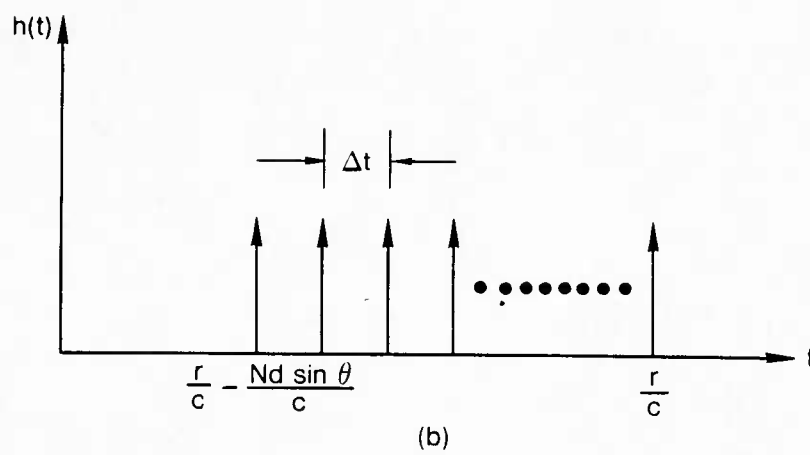
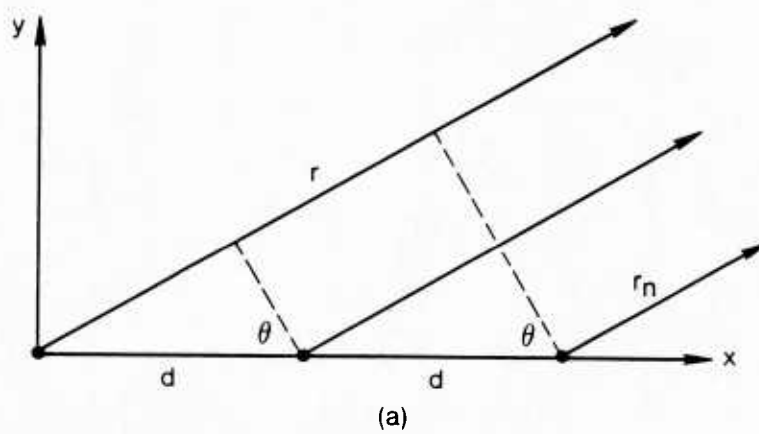


Figure 3-3. Line Array of Simple Sources and Corresponding Impulse Response.

are the times corresponding to the initial and last impulses respectfully.

Thus, the impulse response is a series of impulse functions beginning at time $(r - Nd \sin \theta)/c$, corresponding to the array element nearest the field point, separated by $\Delta t = (d \sin \theta)/c$, and ending at $t = r/c$, as illustrated in figure 3.3(b).

The transient pressure response can be computed as a function of θ according to

$$p(\vec{r}, \theta, t) = \rho \frac{\partial}{\partial t} q(t) * h(\vec{r}, \theta, t) \quad (3.4)$$

If $q(t)$ is a pulsed harmonic function with a time duration $T_D > Nd \sin \theta/c$, a steady state solution will be realized at times greater than r/c . For example, let $q(t) = \text{Re} \{Ae^{i\omega t}\}$ for $t \geq 0$. Then for $t \geq r/c$ the pressure is

$$p(\vec{r}, \theta, t) = \text{Re} \left\{ \frac{\rho c k A}{4\pi r} \left[e^{i\omega(t - \frac{r}{c} + (N-1)\psi)} + e^{i\omega(t - \frac{r}{c} + (N-2)\psi)} + \dots + e^{i\omega(t - \frac{r}{c})} \right] \right\} ; t \geq \frac{r}{c} \quad (3.5)$$

This expression can be rearranged, $e^{i\omega(t - r/c)}$ factored out such that $\psi = (d \sin \theta)/c$, and rewritten as

$$p(\vec{r}, \theta, t) = \text{Re} \left\{ \frac{\rho c k A}{4\pi r} e^{i\omega(t - \frac{r}{c} + \frac{(N-1)\psi}{2})} \left[\frac{\sin(N \frac{kd}{2} \sin \theta)}{\sin(\frac{kd}{2} \sin \theta)} \right] \right\} ; t \geq \frac{r}{c} \quad (3.6)$$

where in general

$$\sum_{n=0}^{N-1} e^{in\alpha} = \frac{\sin \frac{N\alpha}{2}}{\sin \frac{\alpha}{2}} e^{i(N-1)\alpha} \quad (3.6a)$$

The term of equation 3.6 in brackets is related to the conventional beam pattern expression for a line array of N elements. It is therefore apparent that the impulse response of an array can be used to obtain conventional steady state beam patterns.

It is simply observed that the time interval between impulses in figure 3.3b can clearly be related to a frequency and in fact any multiple of this fundamental frequency will maximize the steady state response for a specified $(d \sin \theta)/c$ as shown in figure 3.4(a). If a frequency is selected such that $f = (2M - 1)/2\Delta t$ the steady state response is zero as one would expect; however, there is a non-zero transient effect as seen in figure 3.4(b).

For reasons which will become important later, it should be noted that the time interval between impulses is constant, therefore, a waveform with a constant period is required to achieve a focusing effect.

If the excitation time t_n for each elemental source is controlled, the resultant impulse response for the farfield is

$$h(\vec{r}, t) = \sum_{n=1}^N \frac{\delta\left(t - t_n - \frac{|\vec{R}_n|}{c}\right)}{4\pi r} \quad (3.7)$$

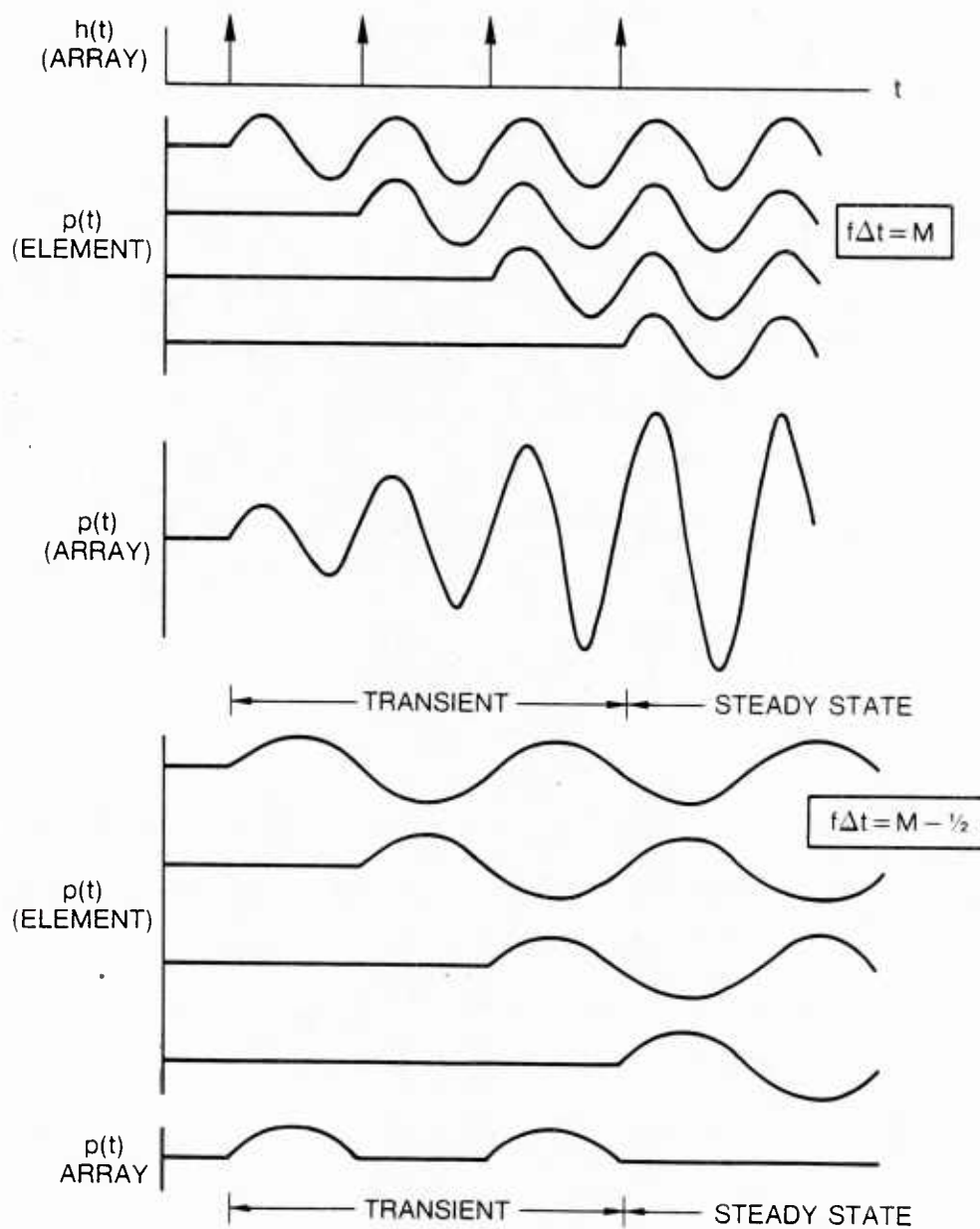


Figure 3-4. Dependence of Transient Array Response on Frequency.

When $t_n = |\vec{R}_n|/c = (nd \sin \theta)/c$ the impulses from all elements will arrive simultaneously and the array is optimally focused. What may not be obvious but is clear from the impulse response function is that the array is focused for all frequencies. Thus, the time delay beamformer is a broadband system.

D. Continuous Line Source

When the general source distribution in space is such that it can be represented as a continuous line source a closed form solution for the impulse response may be formed by a linear superposition of simple sources. Assume the simple sources are of equal strength and uniformly distributed along the x-axis from $x = 0$ to $x = L$. The impulse response Eq. (2.19) may then be written as

$$h(\vec{r}, t) = \int_L \frac{\delta\left(t - t_0 - \frac{|\vec{R}|}{c}\right)}{4\pi|\vec{R}|} dx_0 \quad (3.8)$$

where t_0 denotes the initial excitation time of the source located at x_0 . For reasons which will become obvious let the elemental sources be initially excited according to the linear relationship $t_0 = x_0/v$; v then represents a speed at which a disturbance propagates within the line source. Denoting α as the total time required for a disturbance to reach the spatial point of interest, the impulse response is

$$h(\vec{r}, t) = \frac{1}{4\pi} \int_{\alpha_{\max}}^{\alpha_{\min}} \frac{\delta(t - \alpha)}{\frac{|\vec{R}|}{v} - \frac{(x - x_0)}{c}} d\alpha = \frac{1}{4\pi} \frac{1}{\frac{|\vec{R}(x_0(t))|}{v} - \frac{(x - x_0(t))}{c}} \quad (3.9)$$

where $x_0(t)$ is obtained from the quadratic equation

$$x_0^2 \left(\frac{1}{v^2} - \frac{1}{c^2} \right) + x_0 \left(\frac{2x}{c^2} - \frac{2t}{v} \right) + \left(t^2 - \frac{x^2 + y^2 + z^2}{c^2} \right) = 0 \quad (3.10)$$

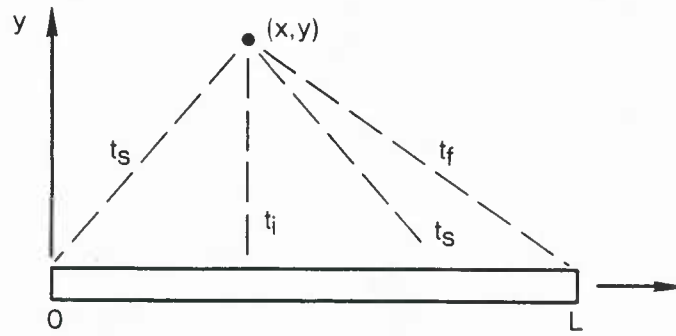
Thus, Eq. (3.9) is quite easy to evaluate numerically if one notes that $0 \leq x_0 \leq L$ and because the equation is quadratic, more than one real solution may exist and both must be included in the solution of Eq. (3.9).

From Eq. 3.9, it is clear the time dependence of the impulse response is dependent on the field point and the speeds of propagation within the source and medium. First consider the case where a continuous line source of length L is uniformly excited, that is the propagation speed in the source is unlimited. The impulse response for this case, obtained from Eq. (3.8) is

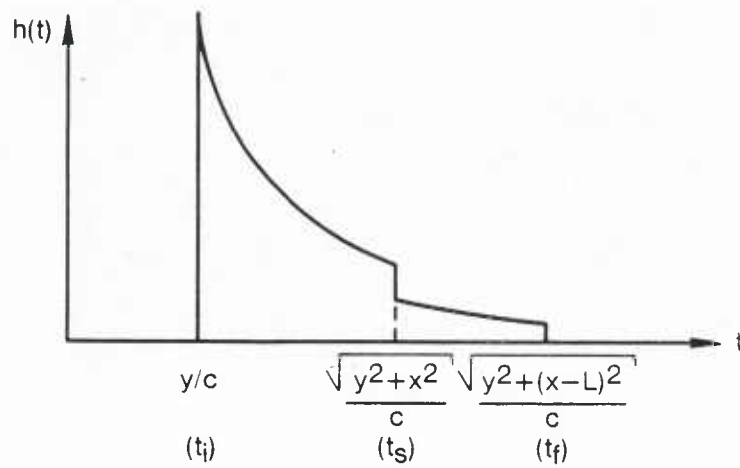
$$h(\vec{r}, t) = \frac{c}{4\pi \sqrt{(ct)^2 - y^2}} \quad ; \quad t > \frac{y}{c} \quad (3.11)$$

and $t_i \leq t \leq t_f$

When the field point (x, y) is located within the region defined by lines normal to the array end points, the impulse response can be evaluated in two parts. The impulse response always begins at $t_i = y/c$; and there are symmetrical elemental contributions to the impulse response until such time (t_s) that the nearest end point of the array has made a contribution as illustrated in figure 3-5(a). The remaining segment of the array is then the sole contribution to the impulse response which persists until the time



(a)



(b)

Figure 3-5. Impulse Response of Continuous Line Source.

$$t_f = \frac{\sqrt{y^2 + (x - L)^2}}{c} ; x < \frac{L}{2}$$

or

$$t_f = \frac{\sqrt{y^2 + x^2}}{c} ; x > \frac{L}{2} \quad (3.12)$$

whichever is greater. The impulse response for this case is shown in figure 3-5(b).

When the x value of the field point is outside the positive half-space region defined by the array the impulse response duration is defined by

$$\begin{aligned} t_i &= \frac{\sqrt{y^2 + (x - L)^2}}{c} \\ t_f &= \frac{\sqrt{y^2 + x^2}}{c} \end{aligned} \quad (3.13)$$

As the distance between the source and field point increase the impulse response becomes shorter in duration and nearly uniform in amplitude; that is, it approaches a rectangular function. If we further restrict the field point location such that $x \gg L$ the impulse response strength is

$$h(\vec{r}, t) = \frac{c}{4\pi |\vec{r}| \sin \theta} ; \quad \begin{aligned} &x \gg L \\ &t_i \leq t \leq t_f \end{aligned} \quad (3.14)$$

The pressure when the source is an impulse is thus

$$p(\vec{r}, t) = \frac{\rho c}{4\pi |\vec{R}| \sin \theta} \left[\delta\left(t - \frac{y}{c}\right) - \delta\left(t - \frac{\sqrt{y^2 + L^2}}{c}\right) \right] \quad (3.15)$$

which except for a factor of 2 is the same as for a planar baffled piston (Stepanishen, JASA, 1971).

Thus far the discussion has dealt with collections of simple sources or a line source. It is now straightforward to replace the single impulse function of a single source with the impulse pair of an extended source so long as the far field assumption with respect to the individual radiators is not violated and care is exercised when evaluating the impulse pair strength and location in time.

The impulse response for an array of identical extended uniformly excited sources and a beamformer when the field point is located in the far field of the individual element may now be written as:

$$h(\vec{r}, t-t_0) = \sum_{n=1}^N \frac{u\left(t - t_n - \frac{y}{c} - \frac{|\vec{R}_n|}{c}\right) - u\left(t - t_n - \frac{\sqrt{y^2 + L^2}}{c} - \frac{|\vec{R}_n|}{c}\right)}{4\pi |\vec{R}_n| \sin \theta_n} \quad (3.16)$$

where θ_n is the angle between the normal to an element and the field point.

The previous development assumed for simplicity that the line source was uniformly excited. Now, consider a simple case of the more general impulse response when the speed of propagation down the source is finite. This translates into a delay associated with the excitation function which is spatially dependent on the source location. As will be shown later, this speed could be associated with the speed of electromagnetic propagation, the speed of a propagating wave in a different medium or a well designed delay line for a beamformer.

Assume the distance from all points on the source is large compared to the source length. From figure 3.6 we note:

$$r_0 = x_0 \sin \theta, \quad R/c \text{ is a bulk delay}$$

and the point on the array x_0 is energized at time $t = t_0 = x_0/v$.

Defining

$$n = 1/v - \sin \theta / c, \quad (3.17)$$

The impulse response function for this system is from equation (3.8)

$$\begin{aligned} h(r, t) &= \int_0^L \frac{\delta\left(t - \frac{R}{c} - \left(\frac{x_0}{v} - \frac{r_0}{c}\right)\right)}{4\pi R} dx_0 \\ &= \frac{1}{4\pi R} \int_0^L \delta\left(t - \frac{R}{c} - nx_0\right) dx_0 \end{aligned}$$

$$\text{Letting } \xi = \frac{R}{c} + nx_0$$

$$h(\vec{r}, t) = \frac{1}{4\pi R n} \int_{\frac{R}{c}}^{\frac{R}{c} + nL} \delta(t - \xi) d\xi = \frac{1}{4\pi R n} \left[u\left(t - \frac{R}{c}\right) - u\left(t - \frac{R}{c} - nL\right) \right] \quad (3.18)$$

This time limited function has three regions of particular interest dependent on the value of n .

When $n > 0$, the leading edge of the impulse arises from the source point farthest from the field point and the trailing edge location is dependent on the values of v , c and θ (see fig. 3.7). That is, the path directly through the medium is the fastest.

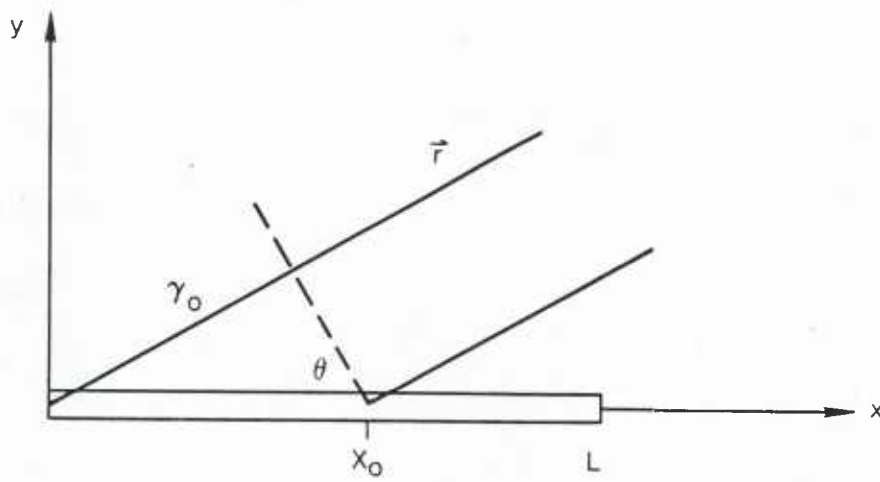


Figure 3-6. Farfield Geometry for Continuous Line Source.

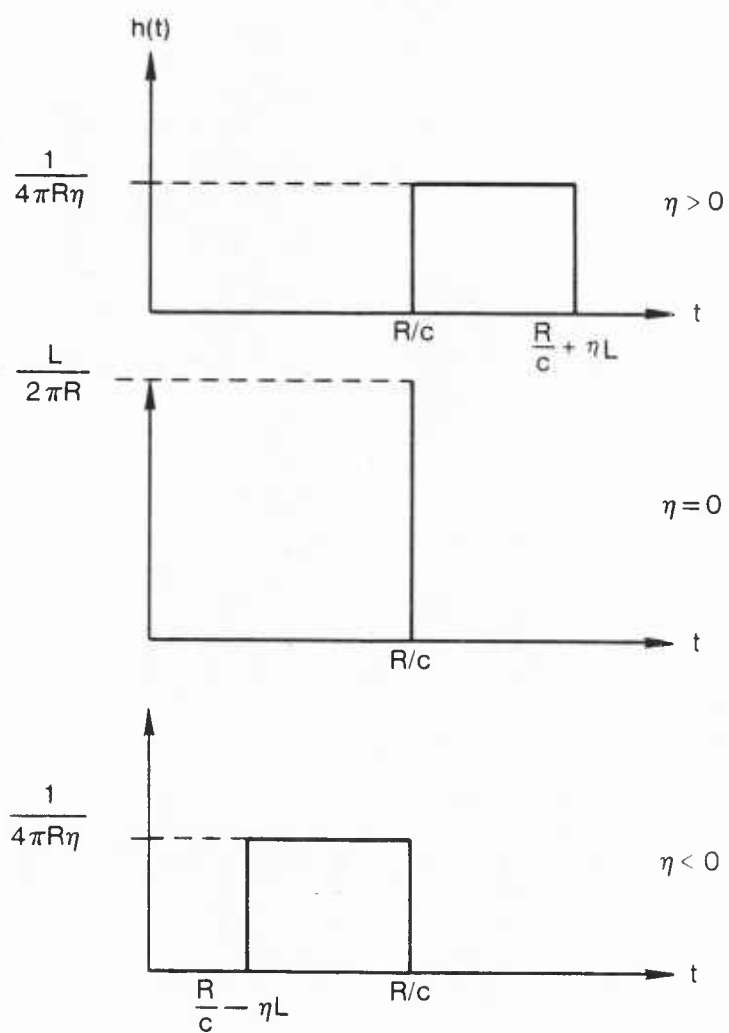


Figure 3-7. Impulse Response of Continuous Line Source as Function of η .

When $n < 0$, the reverse is true and the leading edge is dependent on v , c and θ so it is faster to travel down the source than through the media to the field point.

When $n = 0$, then $\sin \theta = c/v$, and along this radial in the farfield all elemental point sources contribute at the same time thus forming a single impulse at $t = R/c$.

To change the direction for the focused beam the value of v can be changed. This is not generally practical, however, from the impulse response function it is apparent that what is needed to transform the impulse response of the array to an impulse function, which is equivalent to focusing, is to have $nL = 0$. Because L cannot be zero n must be set equal to zero. Noting that $t_D = L/v$ the time delay required to focus an array of this type at a bearing of θ is $t_D = (L \sin \theta)/c$. This equation is entirely equivalent to a phase shifter in narrow band beamformers. The significance of the results is that the proper time delays required for beamforming can be obtained directly from the array impulse response function.

E. Frequency Focused and Scanned Line Array

One further application of the impulse response technique to array system analysis is worthwhile. Consider an electronically focused and scanned line array. This type of array system, often used in acoustic imaging, has been described by Kino (Kino IEEE) and examined in some detail by Souquet et al. (Souquet et al.). They have shown a time dependent frequency signal sent through a delay line can be used for the purpose of electronically focusing and scanning.

Figure 3.8 illustrates the concepts in an array system of this type. The initial excitation time of each element is delayed an amount determined by the delay line speed and element position. The element remains energized for the pulse length. Normally the pulse length is less than the time required for a disturbance to transit the delay line. In effect this results in a subset of elements energized at any instant of time. This subset forms an active array which transmits the array elements at speed v . This is the basis of a scanned array.

For focusing, a Linear Frequency Modulation (LFM) chirp signal of the form

$$e(t) = \text{Re} \left\{ \exp [i(\omega_0 t + \mu t^2/2)] \right\} ; \quad 0 \leq t \leq T \quad (3.19)$$

is used in practice as it is easily generated; the exact non-linear chirp required for exact focusing has been developed (Souquet). The instantaneous frequency of the LFM chirp is shown in figure 3.9. It is noted that ω_1 , the mean frequency of the pulse, must meet the condition (Souquet)

$$\omega_1 = 2N\pi v/\Delta x \quad (3.20)$$

if the excited portion of the array is to have a maximum response normal to the array. To focus at a radial distance y from the array requires the LFM slide constant μ be defined as (Souquet, et al.)

$$\mu = \omega_1^2 v^2 / cy. \quad (3.21)$$

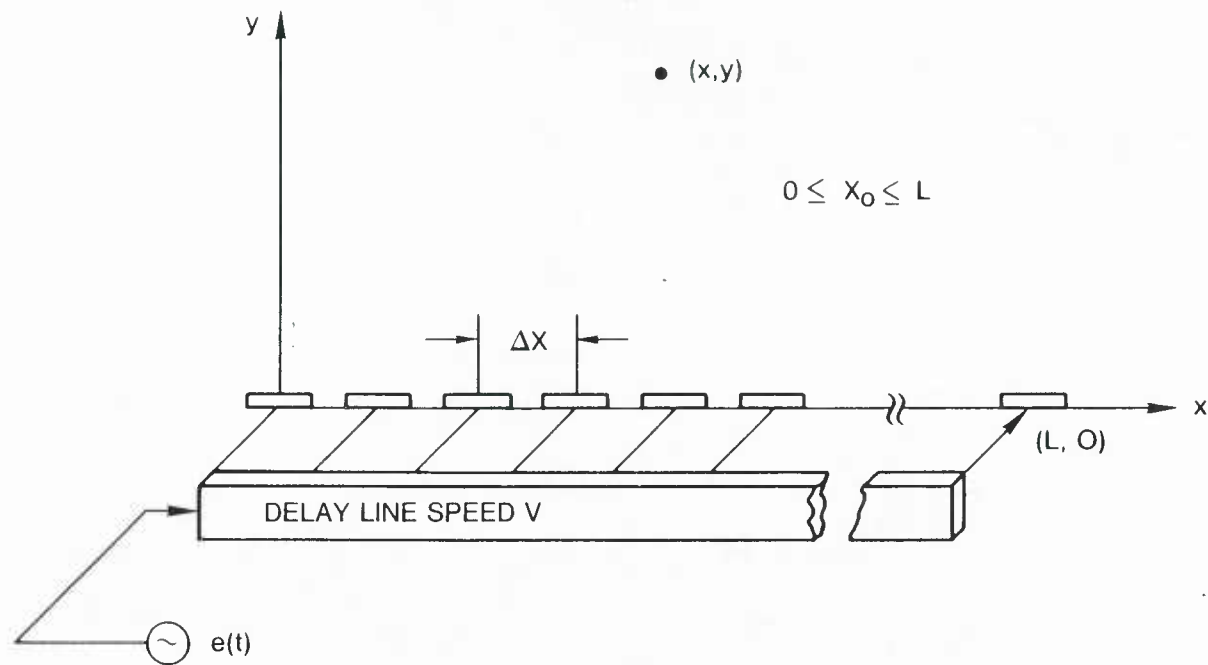


Figure 3-8. Conceptual Diagram of Frequency Focused and Scanned Line Array.

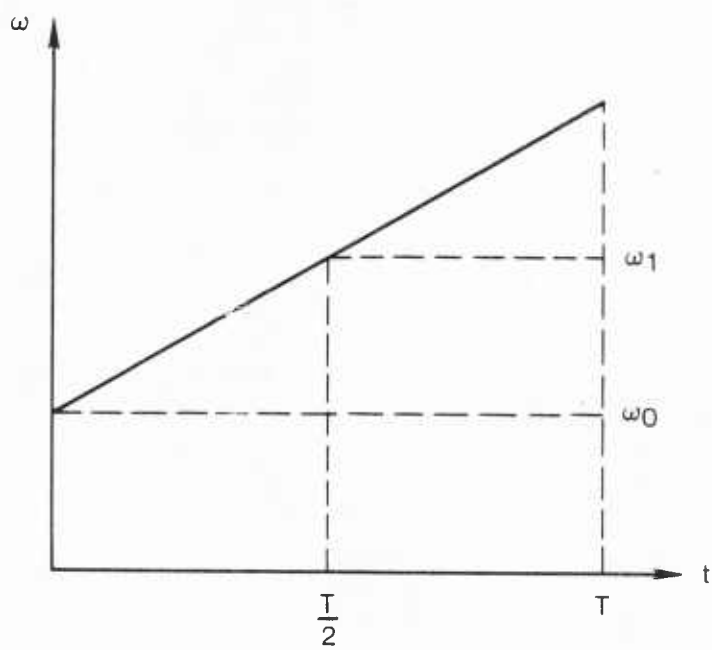


Figure 3-9. Instantaneous Frequency of LFM Chirp.

Thus, the selection of the center frequency, which is dependent on the interelement spacing and delay line velocity, determines the azimuthal angle of the maximum beam while the LFM slide constant determines the range. Note when large focusing ranges are desired μ tends toward zero and the instantaneous frequency required for focusing is constant.

It was of importance to this study to determine if the impulse response technique can be effectively and efficiently used to analyze the same complex array system.

If each element of the array is considered a simple source the discrete impulse response is given by Eq. (2.22) where the beamformer delay is given by:

$$t_n = (n - 1) \Delta x / v = x_n / v. \quad (3.22)$$

The strength of the impulse arising from each element is simply dependent on range. The location of each impulse, found by using Eq. (3.10), is quadratic and may lead under certain conditions to difficulties which are addressed in Chapter 4.

Consider now the case when the focal range is large with respect to the entire array length L . The amplitude of each impulse response in this case will be nearly constant. Furthermore, the equation for the arrival time at the focal point from the n th element is approximately

$$t \approx \frac{x_n}{v} + y + \frac{(x - x_n)^2}{2y} ; \quad (3.23)$$

Therefore,

$$\Delta t \approx \left(\frac{1}{v} + \frac{x}{y} - \frac{x_n}{y} \right) \Delta x \quad . \quad (3.24)$$

This equation is linear in x_n and in the neighborhood where $x = x_n$ Eq. (3.24) reduces to

$$\Delta t = \frac{\Delta x}{v} \quad . \quad (3.25)$$

Recalling (fig. 3.3) the frequency required for focusing is inversely proportional to Δt , the frequency needed to focus this array system is $v/\Delta x$. This is the same constraint imposed by Souquet (Eq. (3.20)).

For a sample point in the farfield the scanning process is achieved with a short cw pulse traveling down the array. Applying reciprocity, a pulse moving down the array and illuminating a sample point in space is the same as a stationary pulse in an array and a moving sample point as illustrated in fig. 3.10. It is important to note that neither the source nor receiver are moving but are controlled by switching action. There are no doppler shifts occurring.

For the case illustrated in fig. 3.10(b) the pressure response in the farfield is

$$p(R, \theta, t) = \text{Re} \left\{ \frac{j \rho c k Q_s e^{-j(kR - \omega t)}}{4\pi R} \frac{\sin \frac{Nkd}{2} \sin \theta}{\sin \frac{kd}{2} \sin \theta} \right\} \quad (3.27)$$

where Q_s is the source strength of an element.

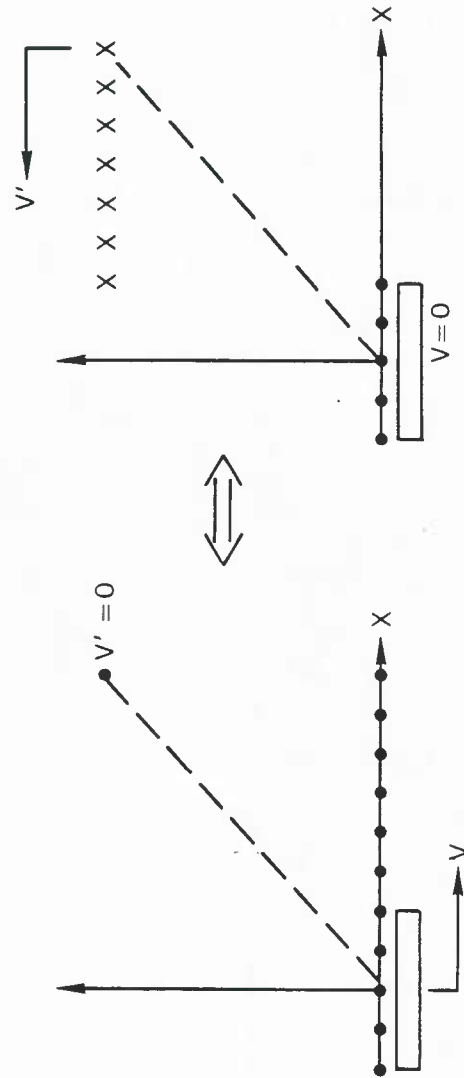


Figure 3-10. Reciprocal Scanning Geometries for a Pulsed Array.

A simple relationship exists between θ and v in this case that is, $R \sin \theta = vt$. Upon substitution and removal of the carrier frequency the envelope of the pressure is:

$$p(R, v, t) = \text{Re} \left\{ \frac{j\omega c Q_s e^{-j(kR - \omega t)} \sin\left(\frac{Nkdtv}{2R}\right)}{4\pi R \sin\left(\frac{kdtv}{2R}\right)} \right\} \quad (3.28)$$

The amplitude of the pressure response in the farfield is of the sinc form with a maximum occurring near the time when $x - x_n = 0$ if the transmitted signal is a cw pulse. This result, based on an analysis of the impulse response function, is the same reached by Souquet, et al.

IV. NUMERICAL RESULTS

A. Introduction

As shown in the previous chapter through the use of several simple cases, the impulse response technique can be used to examine the transient response of array systems. In this chapter the transmit and receive responses of complex systems, comprised of simple and extended sources, such as non-colinear arrays and frequency scanned and focused line arrays are examined. The analysis is done using a computer implementation of the impulse response approach.

B. Continuous Line Array

Consider the case of a continuous line source of finite length. Furthermore, let us assume there is a finite speed, v , associated with the propagation of any disturbance along the length of the source as illustrated in figure 4.1. The impulse response may then be represented in closed form by Eq. (3.9).

Consider first a case when v is very large and the array length is 0.2 m. With the field point located at (0.05, 0.1) and $c = 1500$ m/sec, Eq. (3.9) can be numerically evaluated to obtain the impulse response. The result of this computation is shown in figure 4-2(a). First note the initial strength of the impulse response is very large (observe the vertical scale is disjoint) but rapidly diminishes. During the first 8 μ sec contribution to the impulse response are the result of the elemental sources between $0 \leq x \leq 0.1$ which are symmetrically located about $x = 0.05$ m. The strength of the impulse response from 75 to 120 μ sec is due to the elemental sources from 0.1 to 0.2 m. When the field

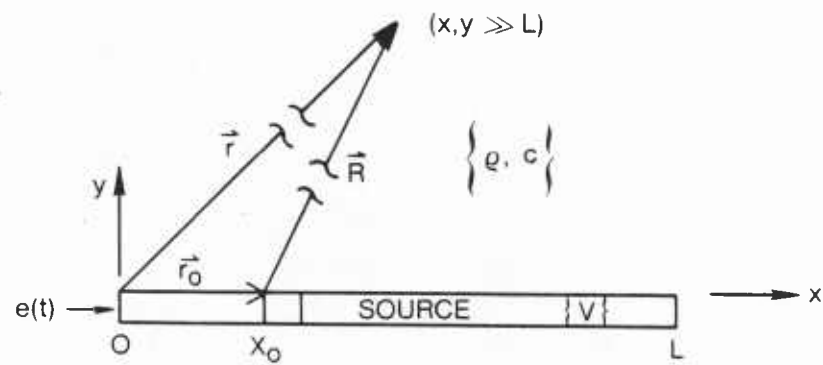


Figure 4-1. Continuous Line Array.

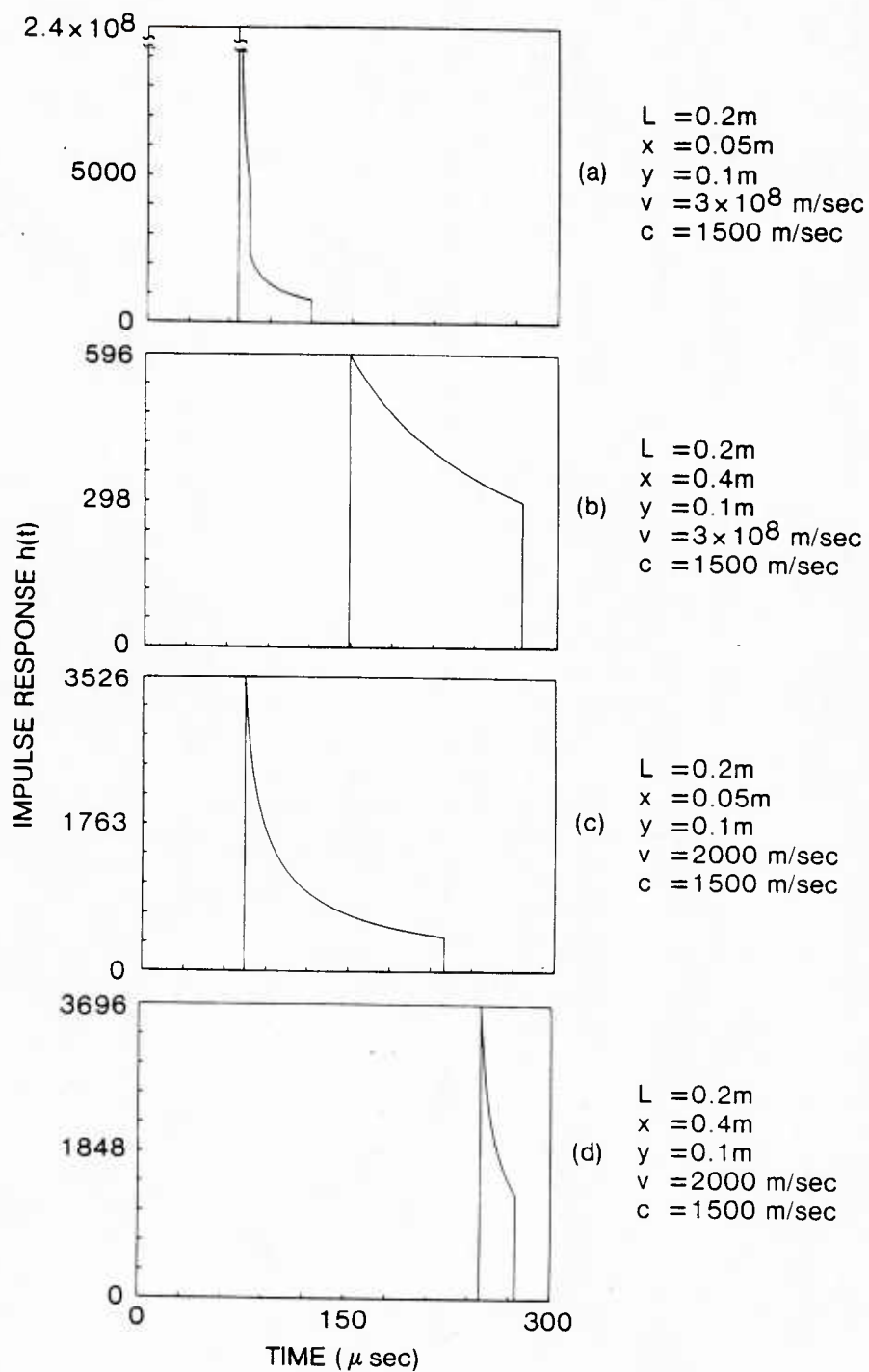


Figure 4-2. Impulse Response of Continuous Line Source with Internal Propagation Speed

point is located outside the region defined by the array, for example at (0.4, 0.1), the impulse response strength (figure 4-2(b)) at any given time is the result of a single elemental source and thus the function is continuous within the time period defined by t_i and t_f .

As a comparison now consider the same cases except the value of v is substantially reduced to 2000 m/sec. The impulse response, when the field point is located within the region defined by the array is presented in figure 4-2(c). The response is now a continuous function and the strength is substantially less than when v was very large. When the field point is located outside the region defined by the array the impulse response (figure 4-2(d)) is shorter and the range of strength values is greater than in figure 4-2(c).

Another simple example exists when the field point is located on the array bisector at a distance such that $y \gg L$. The array is then excited at one end, as shown in figure 4.1, by a CW pulse of duration T . The excitation, while traveling down the array at speed v , causes each elemental source to radiate.

For this case the impulse response closely resembles a boxcar function and the duration of the pressure transient is simply equal to the sum of the temporal extent of the excitation and the impulse response.

Consider now a specific case when the array length is 0.2 m with a delay line speed of 2000 m/sec. The focal point selected is (.1, 10.0) thus $y \gg L$. The normalized instantaneous pressure response for this case, when the excitation is a sinusoidal pulse with center frequency of 1 MHz and duration 10 μ sec, is depicted in figure 4-3. The temporal extent of the transient is 110 μ sec, a result of the 100 μ sec impulse

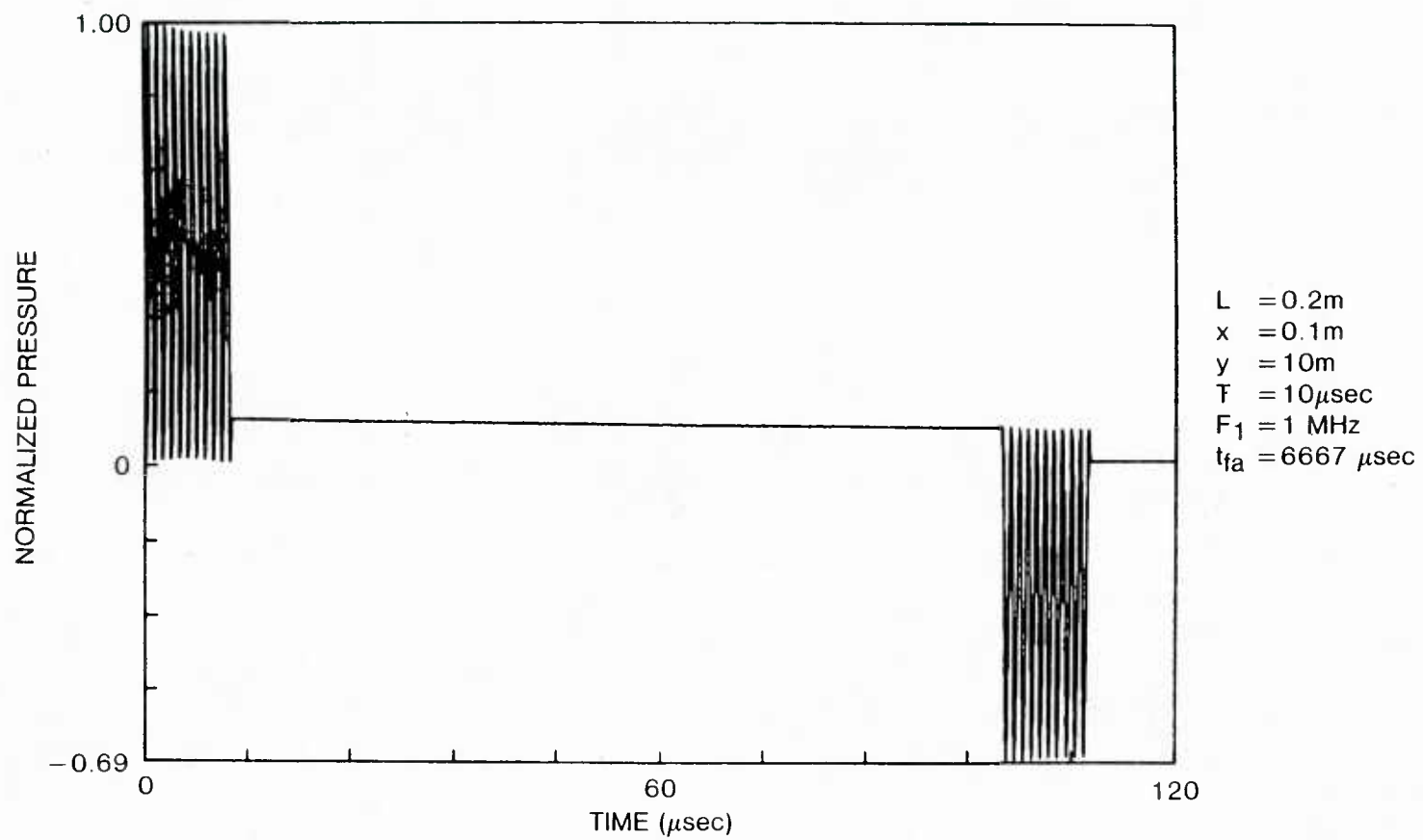


Figure 4-3. Transient Pressure Response of a Continuous Line Array.

response and 10 μsec pulse length. The absolute time of first arrival is also noted on this figure (as it will be in subsequent figures when appropriate) as t_{fa} .

In chapter 3 section D, it was shown the impulse response for a continuous line array is an impulse when the distance to the field point is large compared to the array length and the bearing is $\theta = \sin^{-1}(c/v)$, that is $n = 0$. In this case the far field pressure is simply a delayed, time derivative of the input signal. When n is less or greater than zero the impulse response is spread in time (fig. 3.2) and the resultant pressure response will exhibit temporal dispersion.

Consider the example depicted in figure 4-4 where the array length is 0.2 m and the delay line speed is 2000 m/sec. The three field points of interest lie on the arc of a 10 m circle at bearings such that the three possible ranges of n are examined.

The transient pressure response for a 20 μsec CW pulse at each of the three field points is presented in figure 4-5. When n is greater than zero the time (t_{fa}) at which a disturbance first reaches the field point is associated with the end of the array located at the coordinate system origin. The transient duration is about 55 μsec (fig. 4-5(a)) and a steady state pressure response is never achieved.

In figure 4-5(b), the pressure function appears to be a near replica of the input signal as expected when n equals zero. There is a transient effect near the beginning and end of the response but for the most part this figure represents a steady state solution. The arrival time of the initial disturbance is as expected the same as in the $n > 0$ case. Further it should be noted that the ratio of the pressure amplitudes shown in figures 4-5(a) and (b) is nearly 60:1.

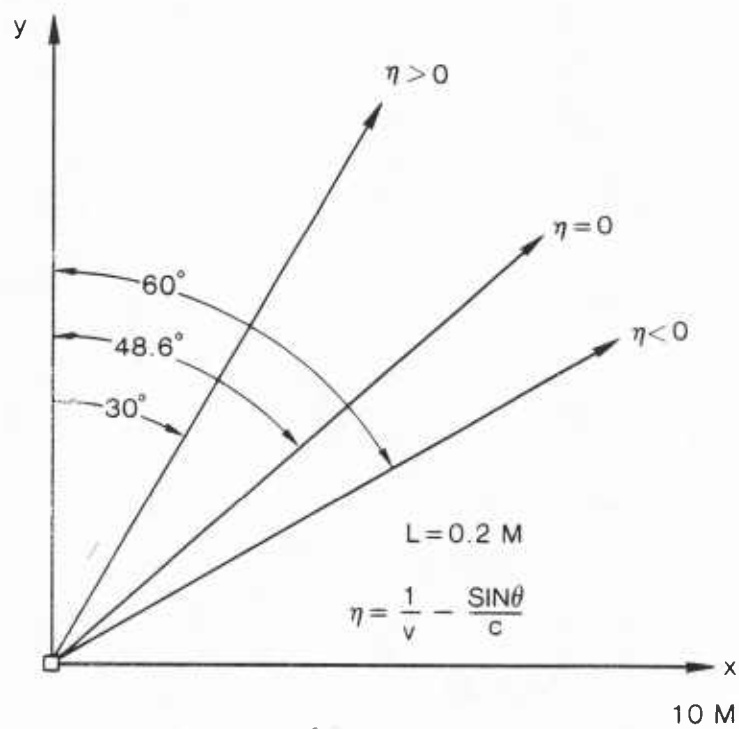


Figure 4-4. Spatial Sampling Points for Continuous Line Array.

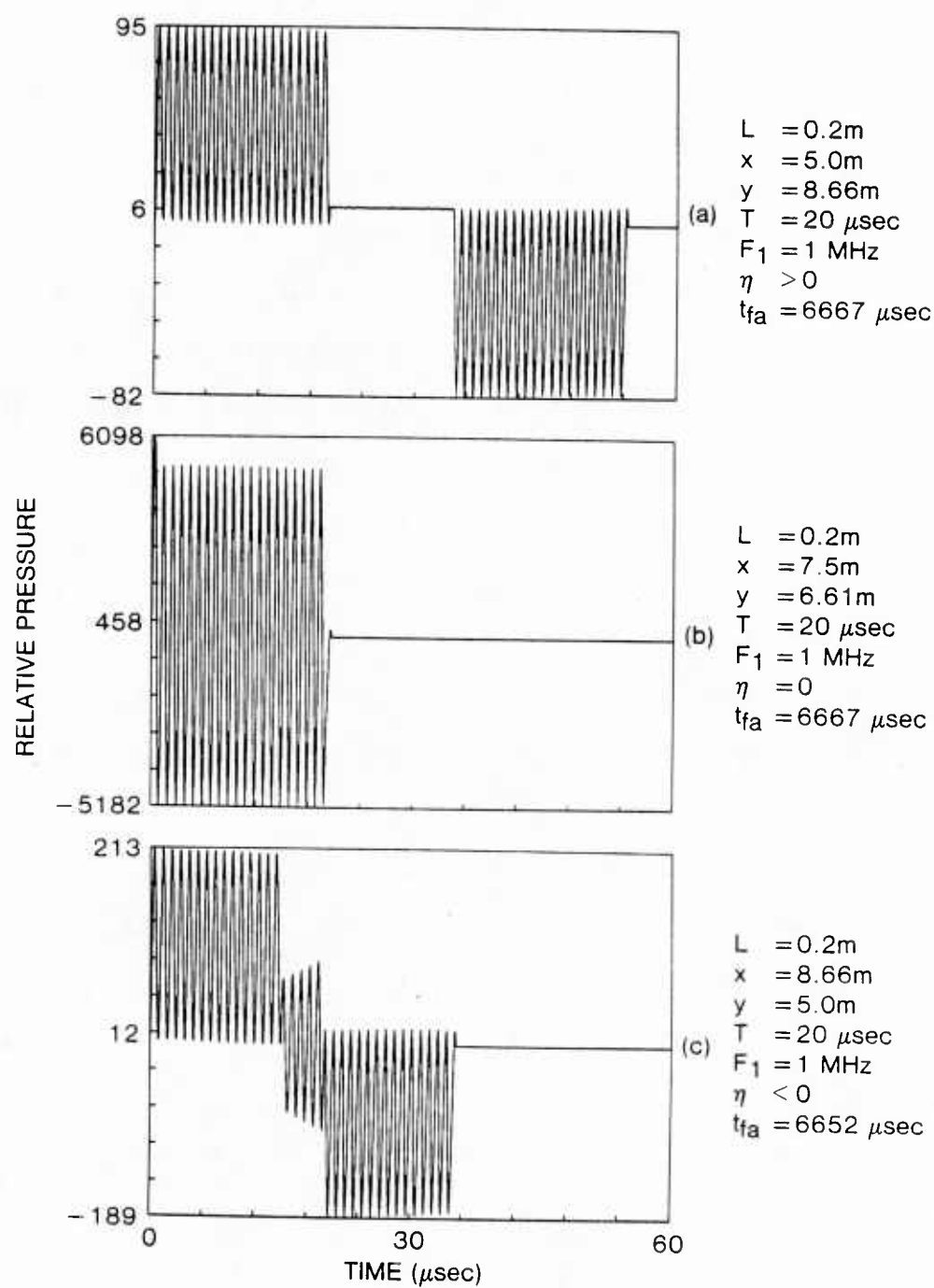


Figure 4-5. Transient Pressure Response for Three Ranges of η .

When n is less than zero, the initial disturbance arises from the end of the array nearest the field point. This means it is faster for a disturbance to travel through the array before entering the media than to travel solely in the media. The transient response begins at 6652 μsec and lasts about 35 μsec so that the end of transient, for the $n < 0$ case, is the same as the beginning of the transient when $n > 0$. In the case for which figure 4-5(c) is presented, a steady state solution exists for about 5 μsec and is noted near the middle of the transient. As in the case for $n > 0$ the amplitude of the transient is substantially less than in the case when $n = 0$.

C. Discrete Line Array

1. Colinear Array of Discrete Elements

Consider an array system composed of linear elements and a time delay beamformer. The individual elements may be simple or extended sources; however, the selection of points is restricted to the far field of the individual elements where the impulse response of the individual element can be represented as a boxcar function. The impulse response for this system can be obtained from Eq. (3.16).

As a simple example, consider the five element colinear array and beamformer illustrated in figure 4-6(a). If the beamformer is removed by setting all time delays in Eq. (3.16) to zero the derivative of the transmit impulse response at the field point is as shown in figure 4-6(b). The strength of the positive and negative impulse pairs is determined by the distance between the center of the element and the x coordinate of the field position. When this distance is less than $L/2$ (on-axis case) the strength is, from Eq. (3.11), $c/4\pi L$. The location

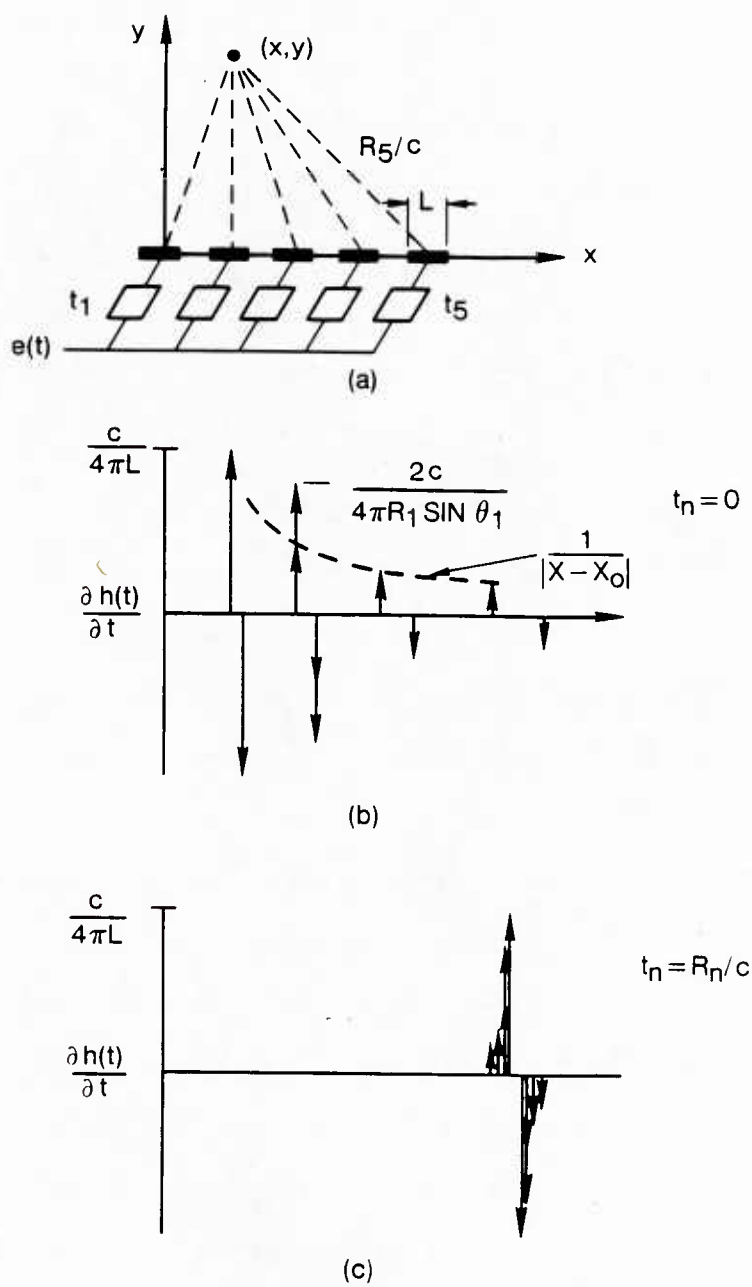


Figure 4-6. Time Derivative of Impulse Responses for Five Element Array With and Without Beamforming.

of each impulse in the time domain is determined by the element location and spatial extent L . With the field point located directly above the second element, the impulses from elements 1 and 3 are colocated and simply summed using linear superposition as indicated by the stacked arrows of figure 4-6(b).

When the beamformer is used to focus the array at the field point by setting $t_n = |\vec{R}_n|/c$ the temporal spread caused by the element location with respect to the field point is removed. The temporal spread caused by the spatial extent of the elements still exists as shown in figure 4-6(c). That is to say, as expected, the directional characteristics of the elements are not removed. Therefore, if the total time spread of the array impulse response shown in figure 4-6(c) is small compared to the highest frequency component of the input time function and the pulse duration is greater than the impulse spread, a steady state solution approaching an ideal array output will be obtained.

The transmit and receive transient response of more complex colinear arrays can now be examined. Consider the array system of figure 4-7. This 35 element array has an interelement spacing of 3 mm and elemental lengths are 1.5 mm or one wavelength at 1 MHz. The array is focused at the focal point (.03, .09). The derivative of the impulse response at four field points along the line $y = .09$ are shown in figure 4-8(a-d). As the field point approaches the focal point, the temporal dispersion of the impulse function decreases and there is some reordering of the arrival structure. Large differences in the strength of the impulse pairs occur because the effects of spreading and element directivity are included in the impulse response.

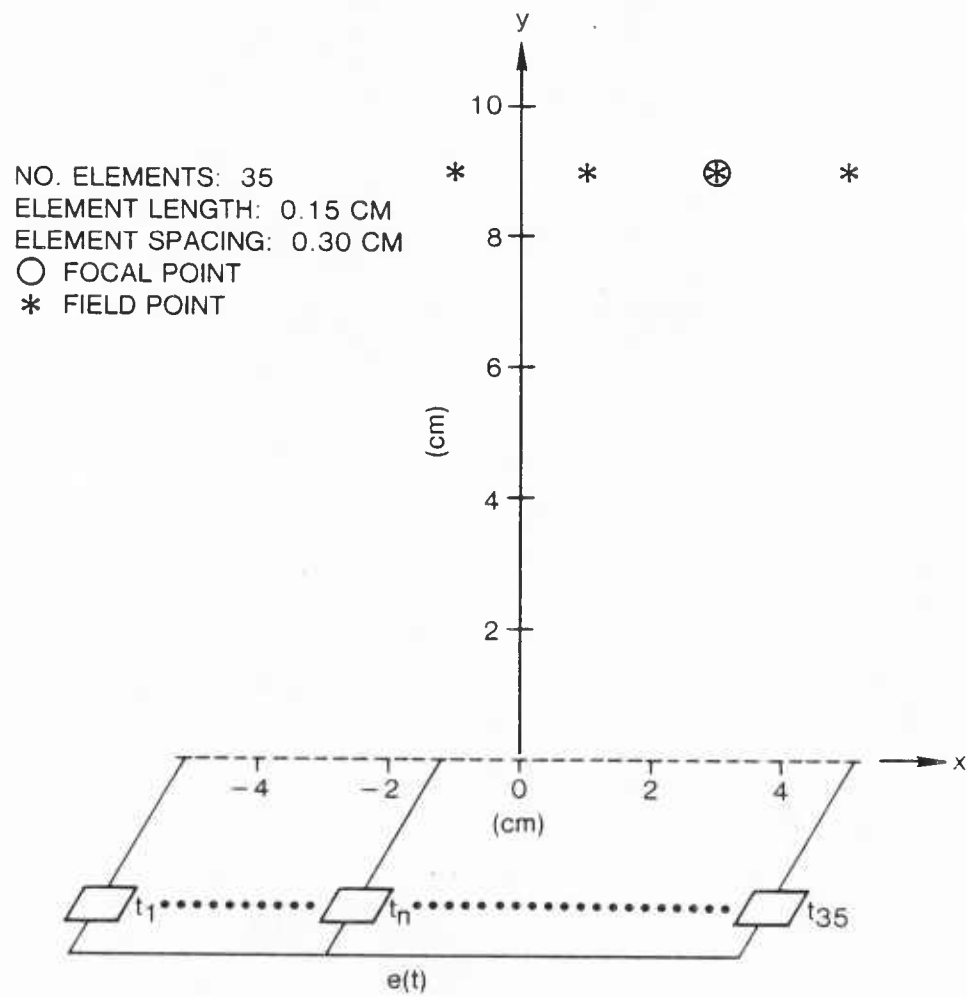


Figure 4-7. Conceptual Diagram of Thirty-Five Element Colinear Line Array and Beamformer.

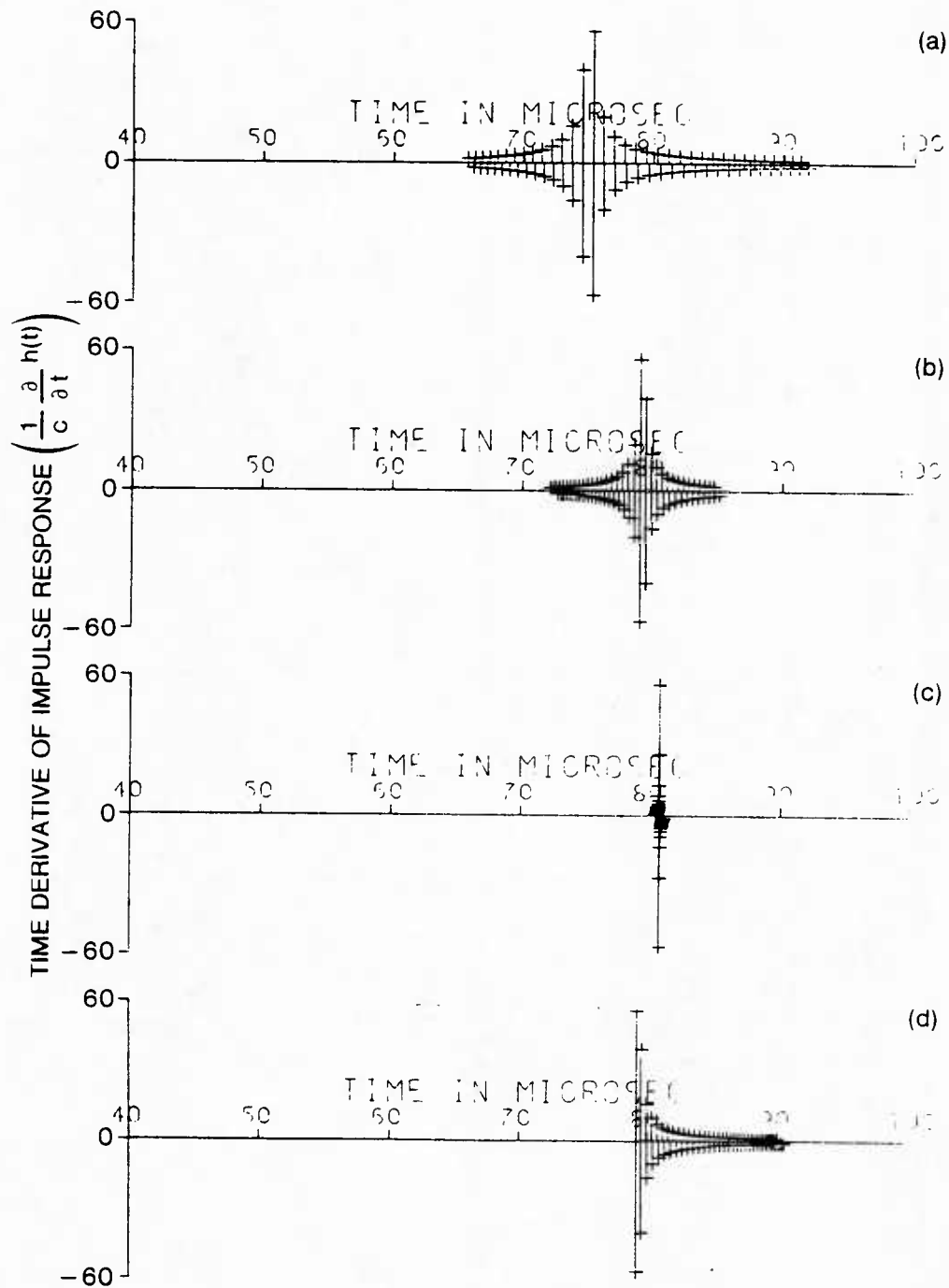


Figure 4-8. Time Derivative of Colinear Array Impulse Response for Four Field Points.

The transient transmitted pressure response for this array system excited by a 20 μ sec CW pulse is shown in figure 4-9(a-d). The time dependent structure of the pressure at field points other than at the focal point is quite complex. This is due to the interference created by the individual elements and beamformer. It is easy to see in figure 4-9 that a steady state solution is achieved near the center of each pattern in figures 4-9(b-d) but the magnitude of the level is substantially less than at the focal point. The pressure at the focal point exhibits some degradation because of the directional (temporal spread) characteristics of the individual elements. This is also the cause for transient effects noted near the beginning and end of the pressure response in figure 4-9(c).

2. Curved Array of Discrete Elements

Now consider a somewhat more complicated array system in which the elements of finite extent are tangent to a smooth curve such as the ellipse in figure 4-10. The impulse response is still obtained from Eq. (3.16); however, care must be exercised to evaluate the angle between the field point and the normal to the elements as shown in the figure.

For comparative purposes the elliptic array case contains the same number of identical elements and has the same field points and focal point as the previous colinear system. The interelement spacing is non-uniform along the array but linear (3 mm) in the x-direction. The time derivative of the impulse response for the selected field points along the $y = .09$ line are shown in figure 4-11(a-d). When compared with the responses obtained for the colinear array, several interesting

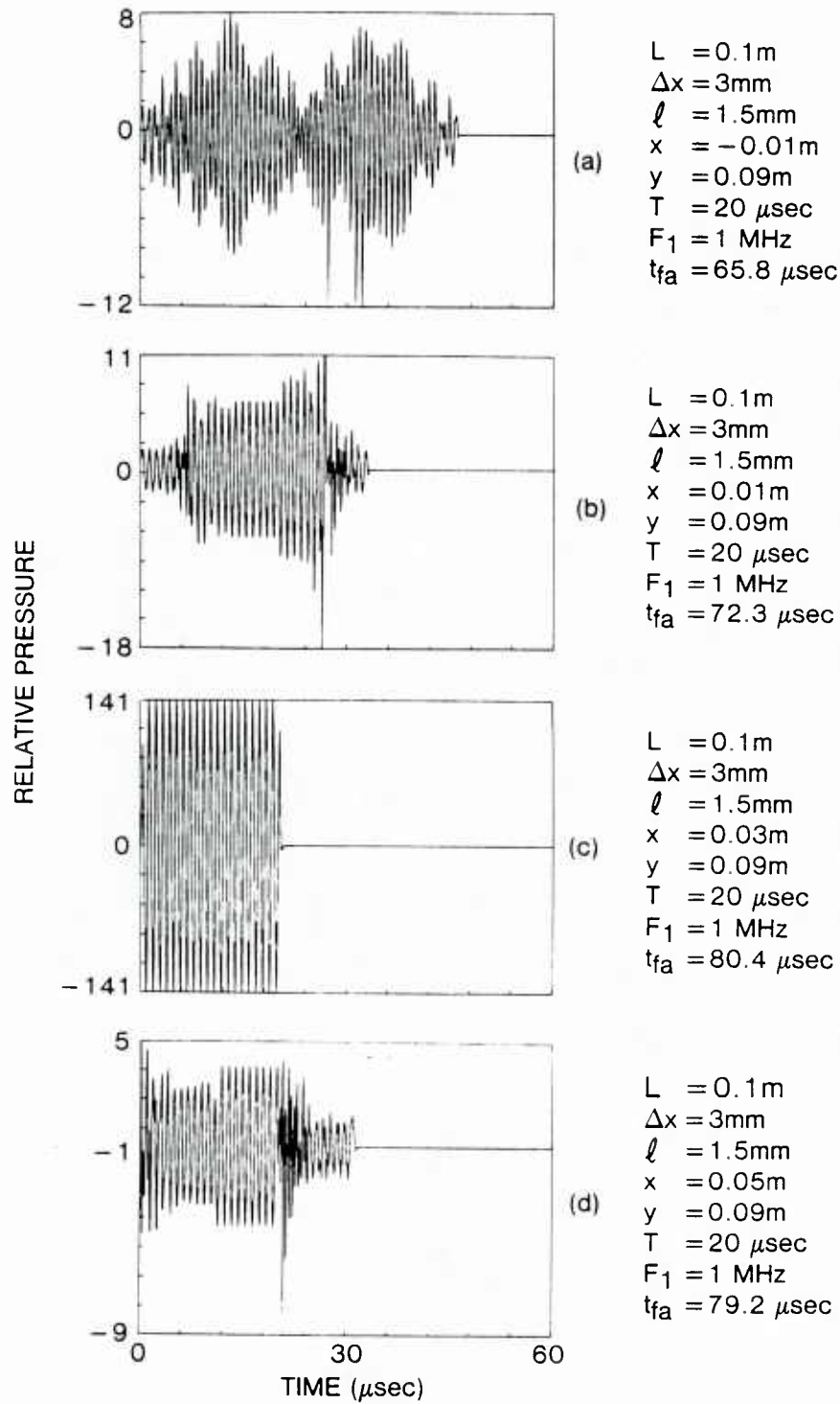


Figure 4-9. Transient Pressure Response of Colinear Array for Four Field Points.

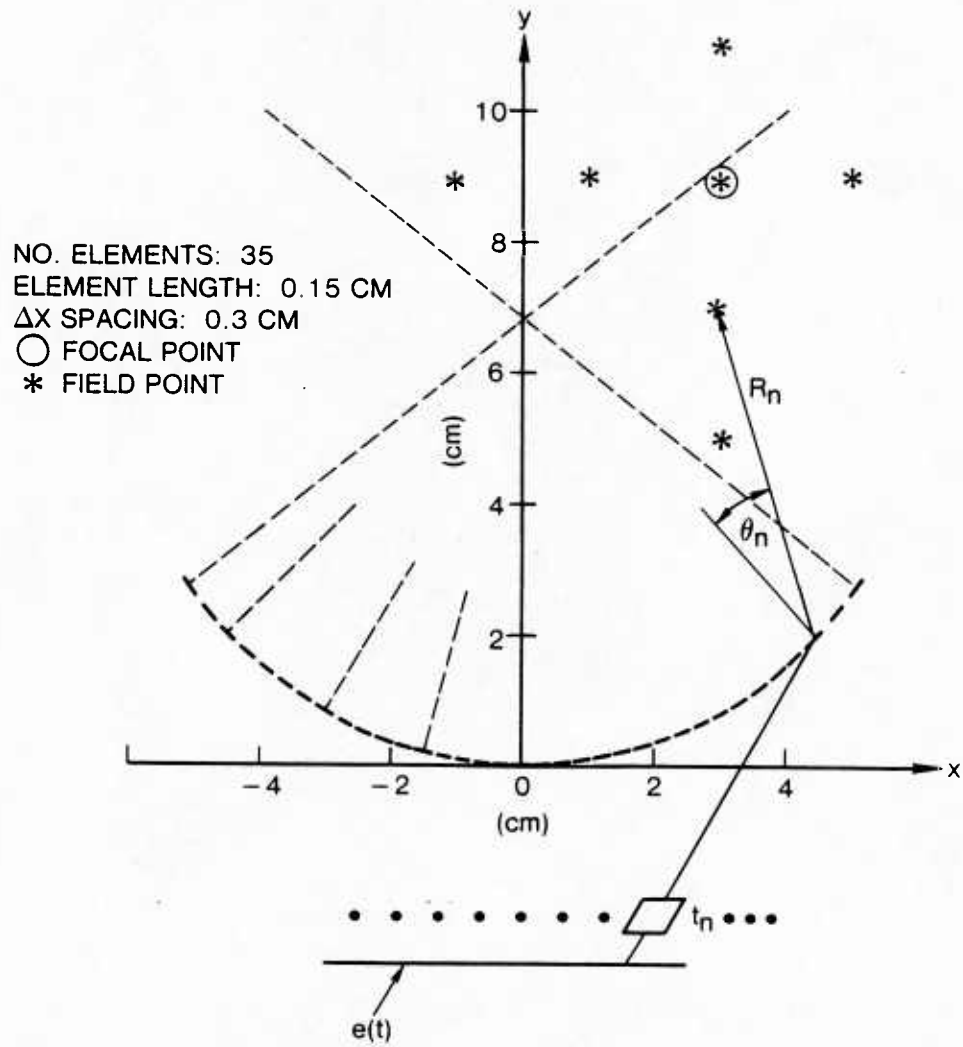


Figure 4-10. Conceptual Diagram of Thirty-Five Element Curved Line Array and Beamformer.

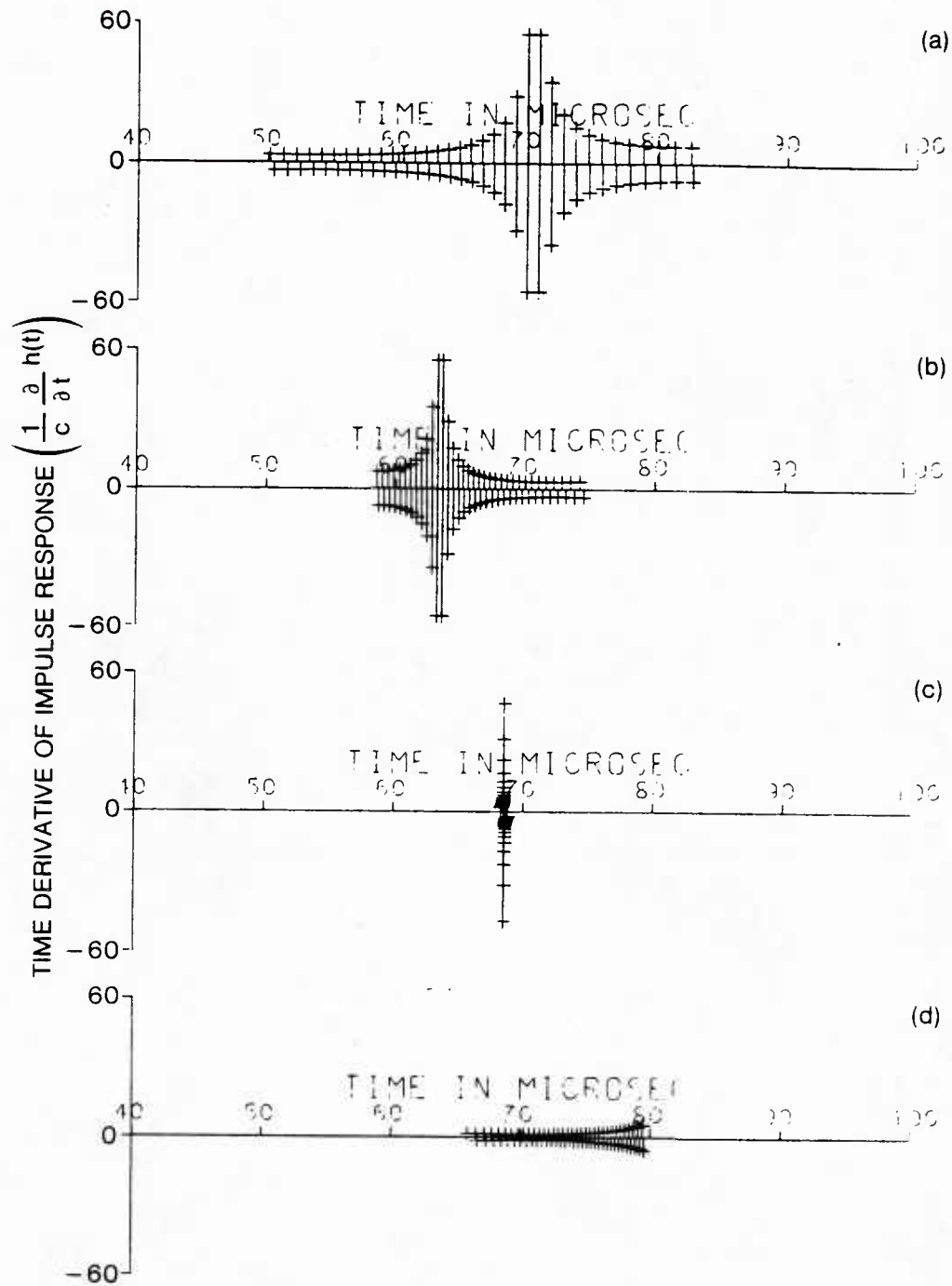


Figure 4-11. Time Derivative of Curved Array Impulse Response for Four Field Points along the Line $y = 9$ cm.

features can be noted. In general the response functions for the first three field points (a, b, and c) are similar in nature and the differences in strength and temporal width are not very great. A perusal of the response functions for the focal point reveals that, although the time delay beamformer has colocated the impulse pairs in the colinear and curved array systems, the geometric curve of the ellipse has reduced the time spread caused by the individual elements and thus provides better system performance.

It is also interesting to note there are substantial differences in strength between the impulse functions presented in figures 4-8(d) and 4-11(d). This is because in the elliptic array the last field point illustrated is not within the region defined by the long dashed lines in figure 4-10. These lines, normal to the end elements of the array, define an area within which the angle between the field point and an element normal becomes small for one or more elements.

The transmit pressure responses obtained from the impulse functions of figure 4-11 and a 20 μ sec CW pulse of frequency 1 MHz are presented in figure 4-12 for completeness.

Figure 4-13 illustrates similar results for field points along the line $x = .03$. The impulse values for the first two field points are low despite their proximity to the array because these points are outside the region defined by element normals. Steady state solutions are observed in the transient pressure responses of figure 4-14 because in each case the pulse length exceeds the duration of the impulse responses.

It is interesting to note that for certain source functions low amplitude pressure fields can exist in close proximity to curved arrays

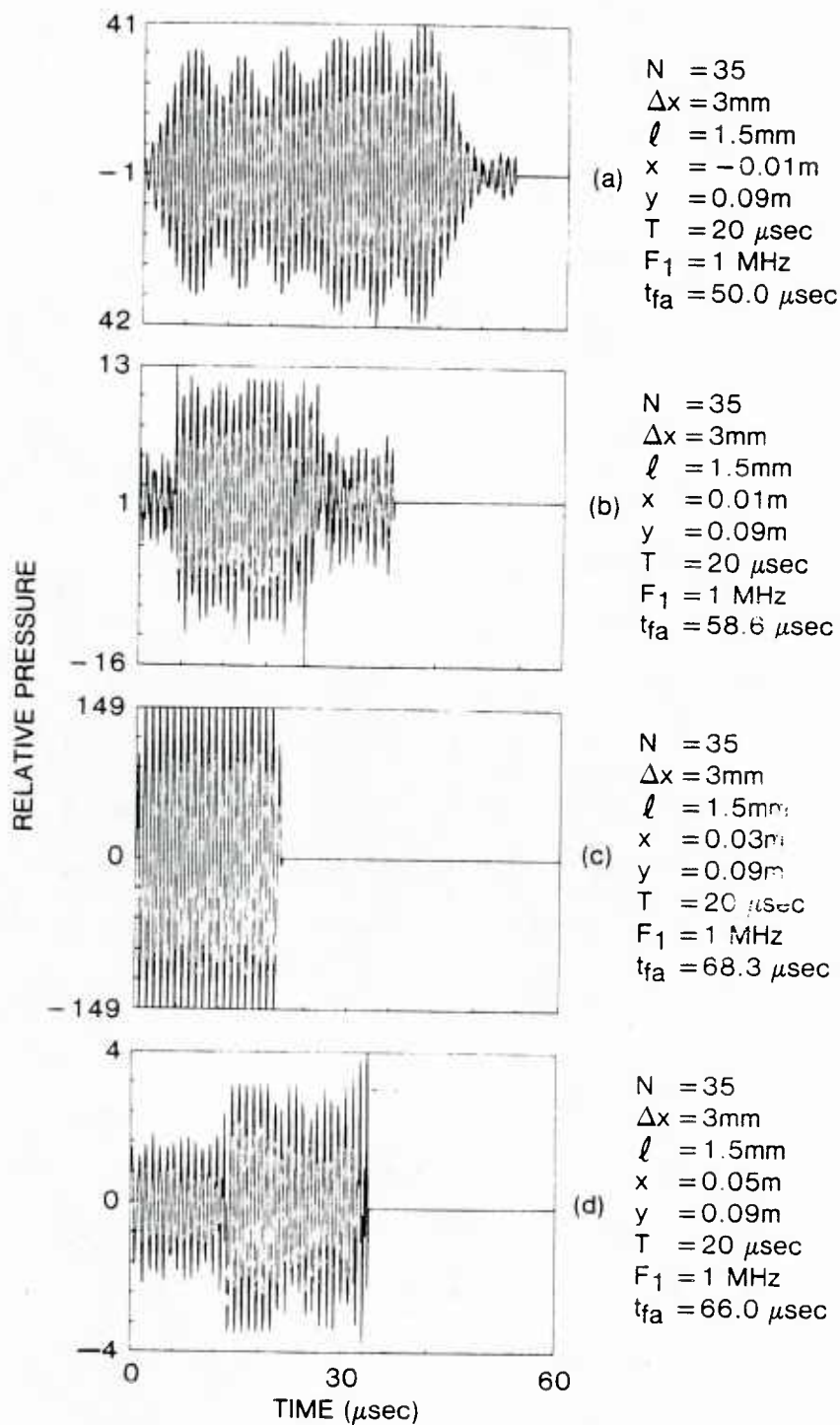


Figure 4-12. Transient Pressure Response of Curved Array for Four Field Points along the Line $y = 9\ \text{cm}$.

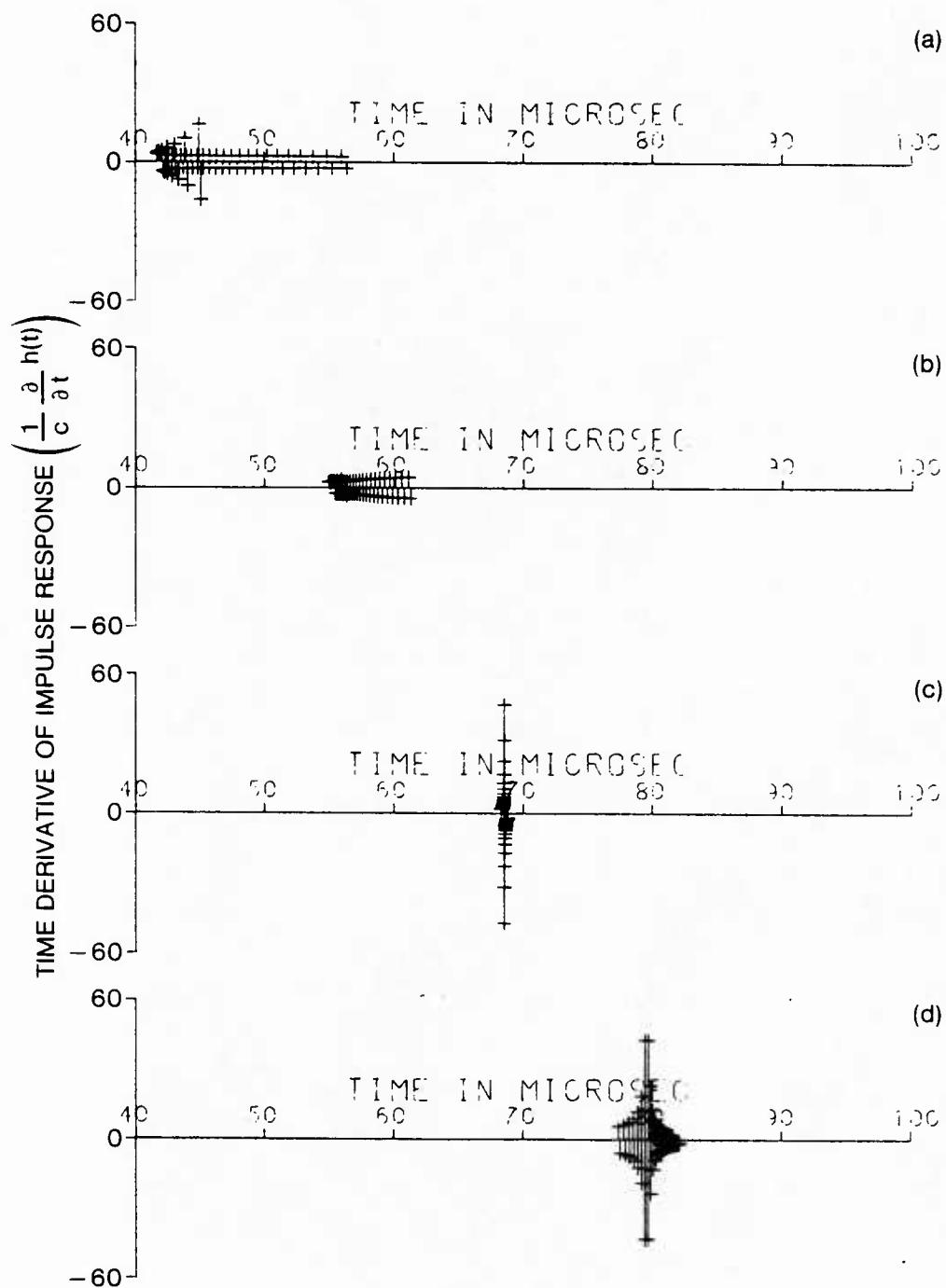


Figure 4-13. Time Derivative of Curved Array Impulse Response for Four Field Points along the line $x = 3$ cm.

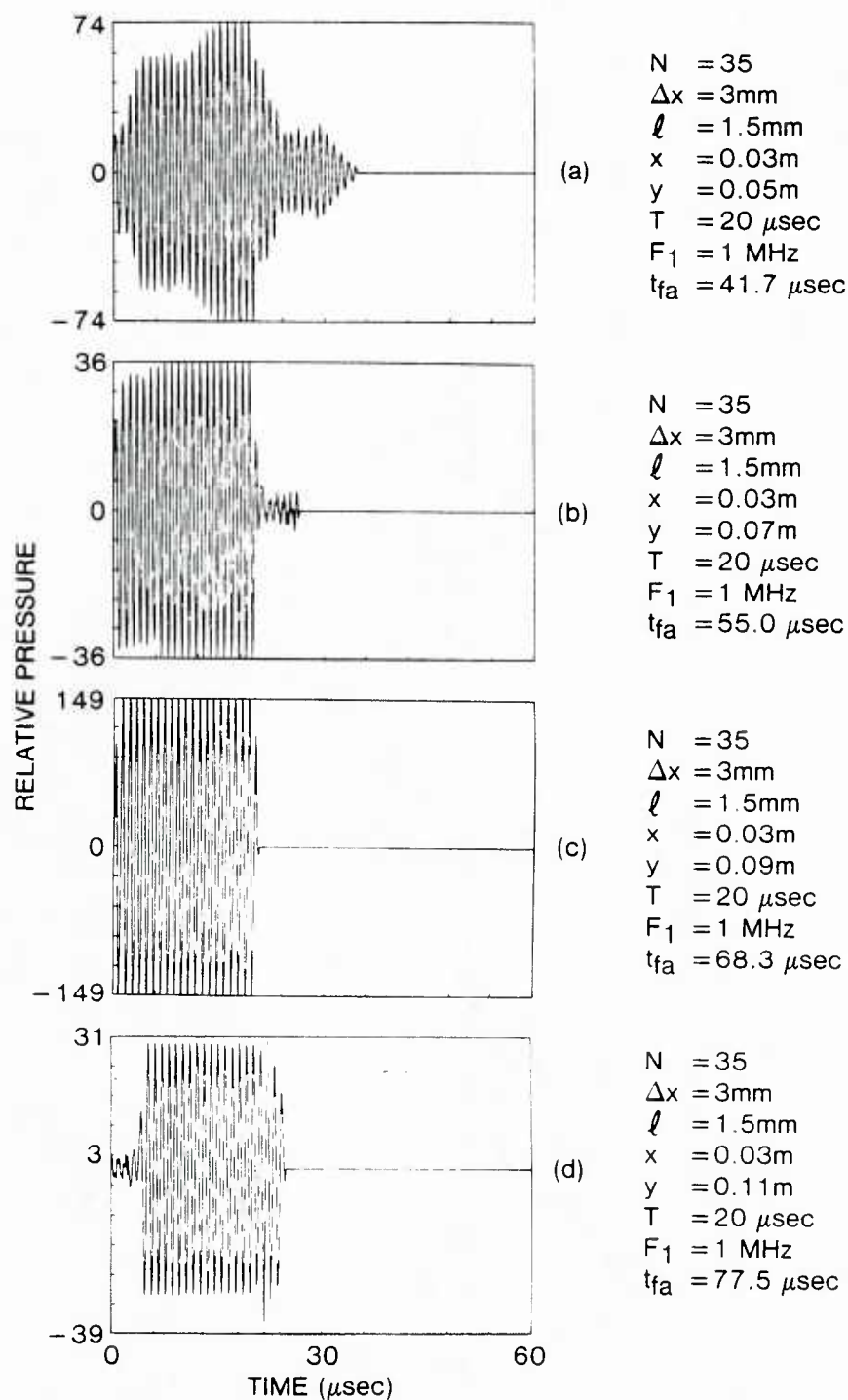


Figure 4-14. Transient Pressure Response of Curved Array for Four Points along the Line $x = 3\ \text{cm}$.

when the field points are outside the region defined by the array geometry, element orientation and spatial extent. Furthermore, curved arrays can further enhance array performance at focal points by reducing the temporal spread caused by element length. There is no improvement, however, in the case when the elements behave as simple sources.

3. Frequency Focused and Scanned Line Array

Consider the frequency focused and scanned line array system illustrated by figure 3.8 when the distance to the focal point is large. In this case the FM slide constant is very small. The instantaneous transient pressure response obtained using the impulse response technique and the indicated variables is shown in figure 4-15(a). Based on the discussion in Chapter 3, the sinc dependence on time is expected. This is a bit more obvious if the instantaneous results are demodulated to obtain the signal envelope and converted to decibels. This was done to obtain figure 4-15(b). It can be noted the ratio of mainlobe to first sidelobe is very near the expected value of 13.5 dB. Also of interest is the slight asymmetry of the response in time and amplitude. This is due to aberration induced by the pulse traveling down the delay line (Souquet).

Consider now the case when the field point is relatively close to array but still at a range such that each element behaves as a simple source. The strength of the impulse response arising from each element is quite simple but its location in time relative to other elements is more complex and governed by Eq. (3.10). This equation is quadratic in

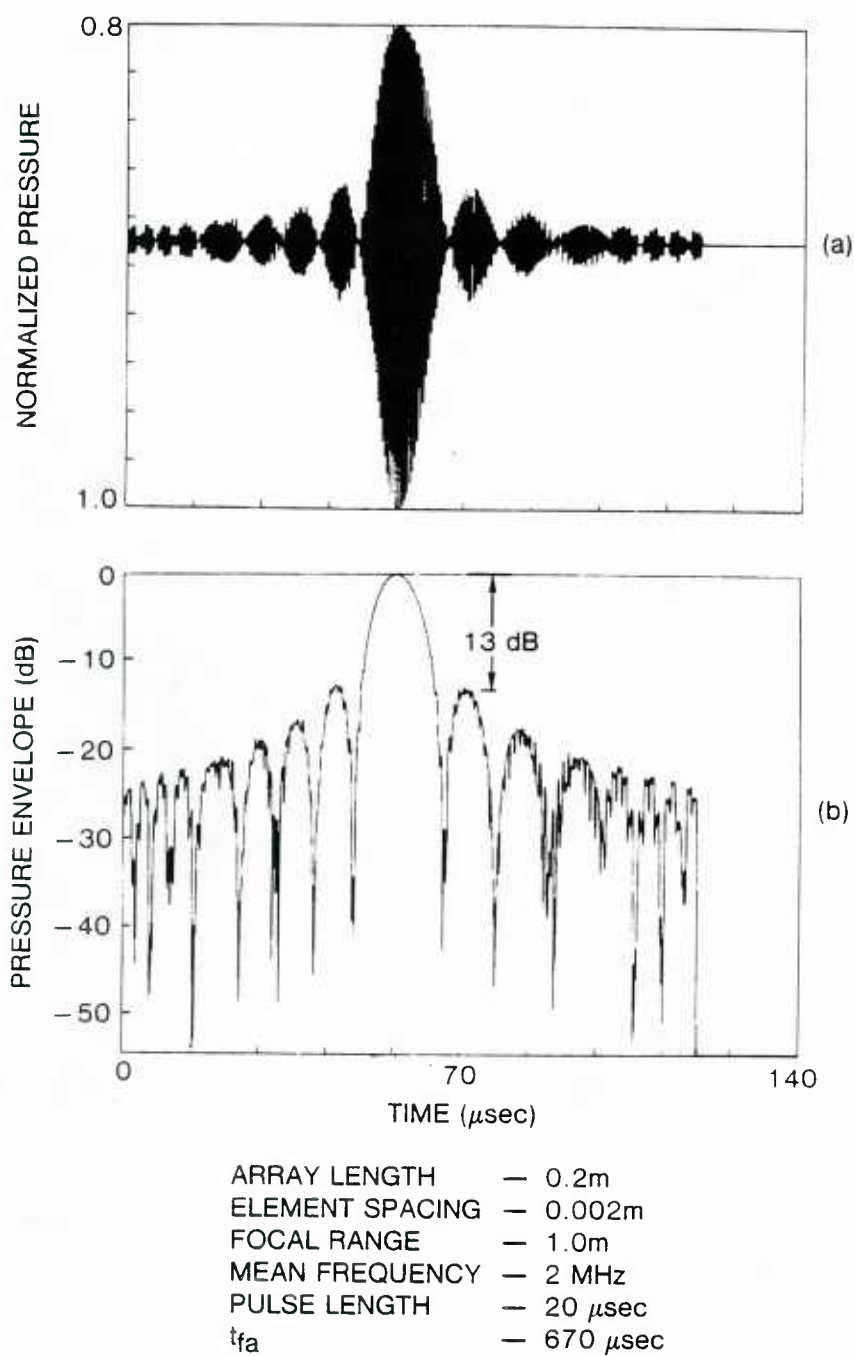


Figure 4-15. Pressure Time Series from Scanned and Focused Array in the Farfield.

nature, thus it is possible to have two disturbances from non-contiguous elements arrive at nearly the same time.

Figure 4-16 is a set of three curves depicting the time required for disturbances emanating along the array to reach the field points. For example, when the field point is located at (.1, .1) it takes about 110 μsec for a disturbance to travel down the array to the element located at $x_0 = .085$ and then through the media to the field point. In the case when the field point is (.2, .1) two elements can contribute to the impulse response at nearly the same time during the first 6 μsec of arrivals. In this case the time when the array is focused at (.2, .1) is outside the time period of double reception, hence the double receptions will not degrade the focusing. However, under certain conditions, for example, higher values of v , when doublets arrive during the focusing period, some degradation in array performance is expected. Because v is finite the doublet pairs will not in general arrive at exactly the same time. The focusing period is defined as the time at which the pulse is centered under the focal point. For example, in fig. 4.16 the focal period when $x = .1$ and the pulse period is 20 μsec is about 130 μsec .

The impulse response for a 100 element array and delay line with an internal speed of 2000 m/sec at the field point (.1,.1) is depicted in figure 4-17. The values were selected in order to compare the results with those obtained by Souquet, et al. In this particular case, the field point is located over the array midpoint, thus, there are as many impulses to the left as to the right of the maximum value. However, the temporal spread about the maximum value is not symmetrical.

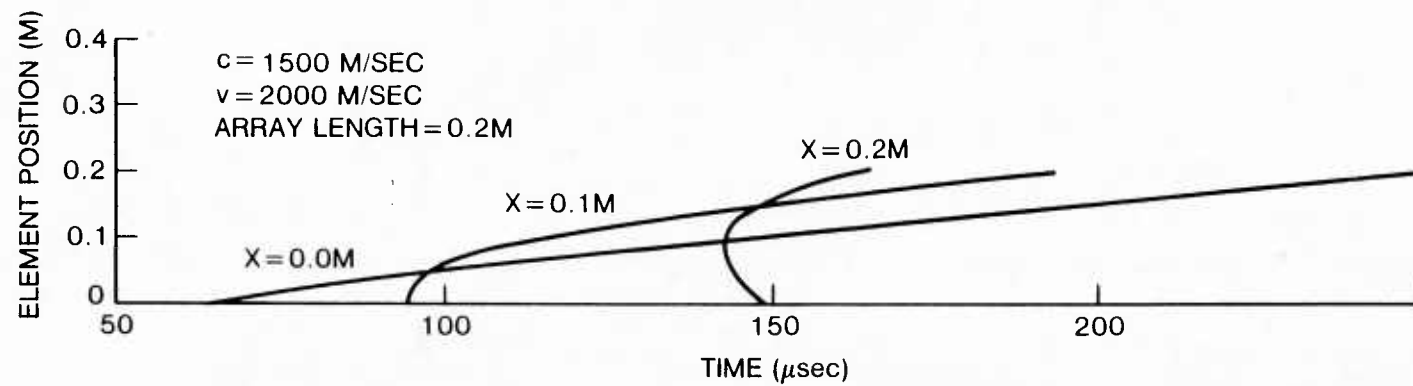


Figure 4-16. Initial Disturbance Time at a Field Point versus Element Position along $y = 10$ cm Line.

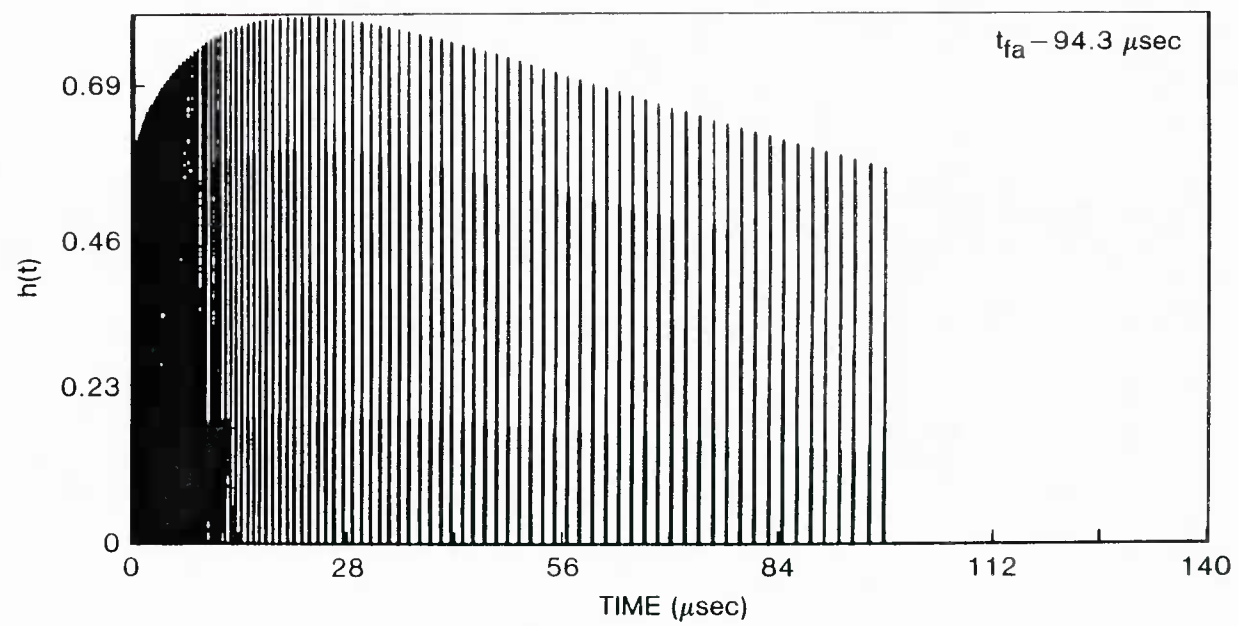


Figure 4-17. Impulse Response for Scanned and Focused Array.

As discussed in Chapter 3 the frequency required to obtain the constant phase values required for focusing can be readily obtained by determining the time between impulses. The solid line in figure 4-18 is a graph of the frequency required at the last 75 out of 100 elements to focus this array at the specified field point.

For a given pulse length only a portion of the array is excited at any given time. If the exact frequency content required for focusing is replaced by an approximation as in the case with an LFM chirp, then a reasonable facsimile of focusing can be achieved. The dashed line represents the LFM chirp selected for focusing based on equations 3.19, 20 and 21. Thus, in the focusing process, the LFM chirp exhibiting the frequency versus time character depicted by the dashed line in figure 4-18 moves down the array at speed v . When the two graphs coincide, focusing occurs at the specified field point. This occurs when the pulse is under the field point. It can be shown by differentiating the argument of the delta function in Eq. 2.22 twice with respect to x_n the slide constant required for focusing when the pulse is located beneath the field point is independent of x and proportional to v^2/cy . This is the same restraint imposed by Sauquet et al.

When the LFM signal selected by Souquet containing a center frequency of 2 MHz is convolved with the impulses of figure 4-17 and differentiated, the resultant pressure field is shown in figure 4-19(a). Figure 4-19(b) is the envelope of 4-19(a) in dB. It is shown here only for comparative purposes and to aid in comparing the results derived here with the results published by Souquet et al. It is clear the array system is focused at the spatial point of interest at a time (126 μ sec) when the pulse is centered in the delay line below the field

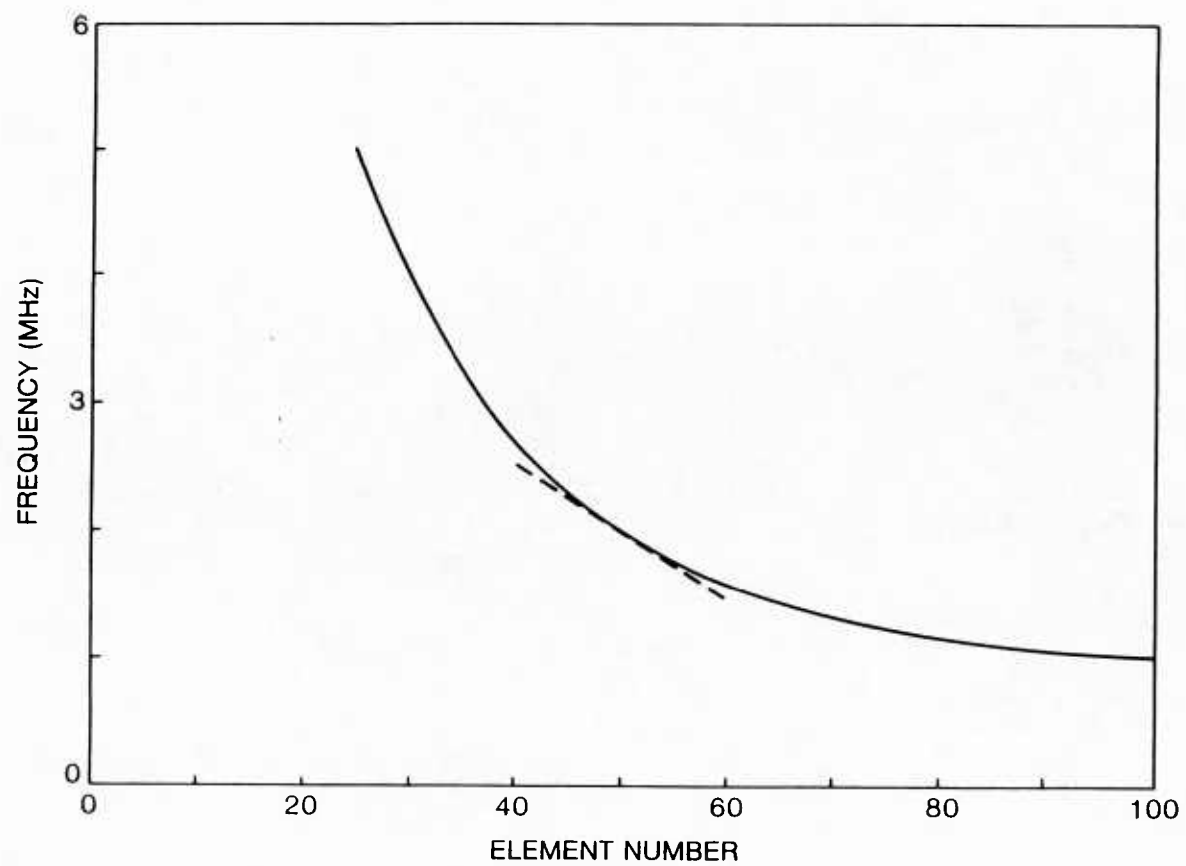


Figure 4-18. Instantaneous Frequency as Function of Element Location Required for Focusing at One Location.

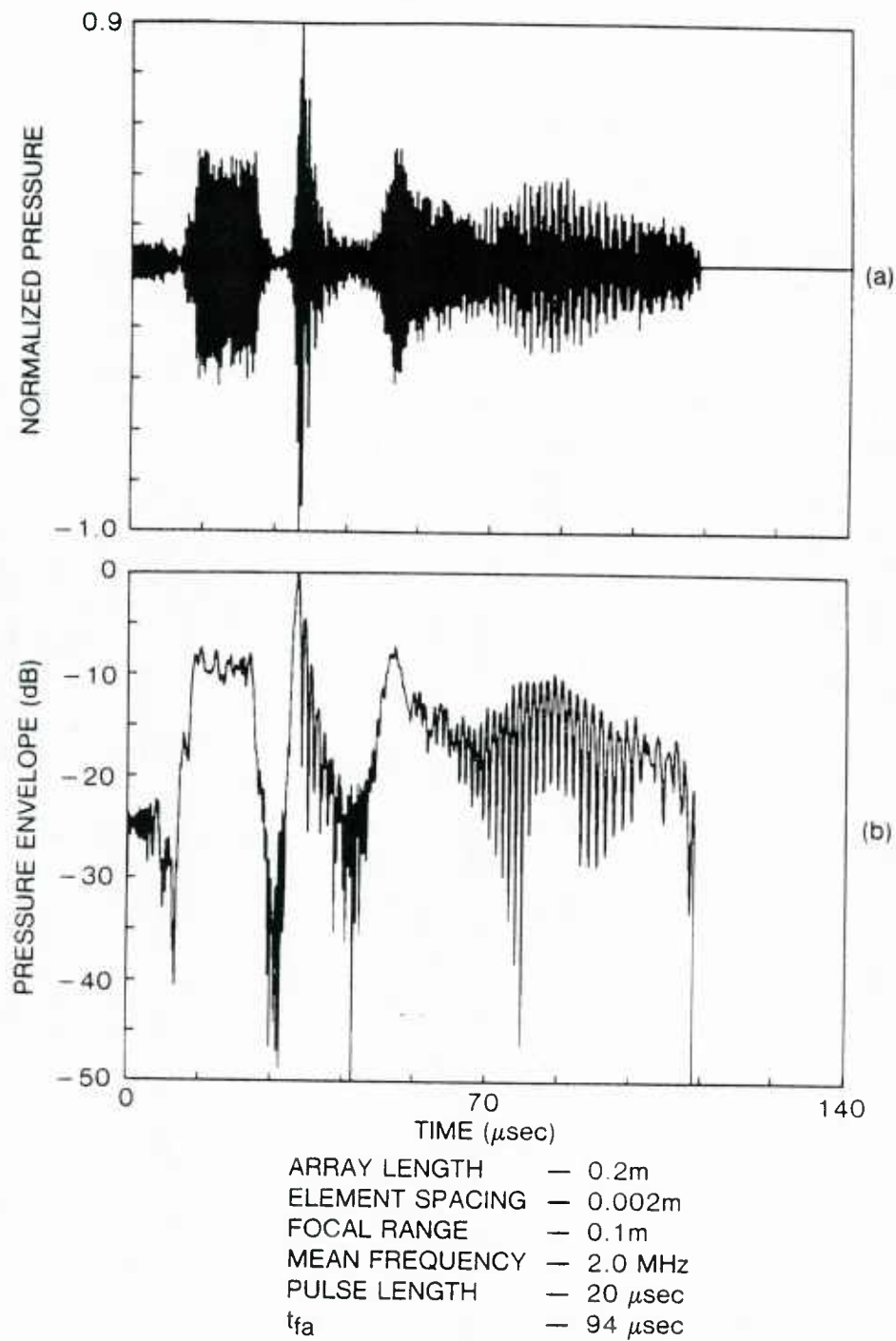


Figure 4-19. Transient Response from a Scanned and Focused Array Using the Impulse Response Technique.

point. There are several other features in the transient pressure response which can be explained on the basis of the impulse response function. As was just shown in the far field case a CW pulse traveling down the delay line leads to a conventional beam response when the interval between impulses is linear (see fig. 4-15 and Eq. (3.28)). Note from the impulse response in figure 4-17 that the temporal samples are non uniformly spaced in time, this is analogous to unequal element spacing (Handbook of Array Technology).

It is well known from antenna design theory that the radiation-pattern of an aperiodic spatial array may be described in three parts (Steinberg). The maximum response region exhibits characteristics for which the array is designed. This is followed by a clean sweep region and then a region of moderately high levels called the plateau region. These regions are then analogous to the time domain response observed in figure 4-19(a) with a few complications. Observe, there is a maximum response at about 127 μ sec, are regions of very low amplitude adjacent to the maximum response and the resemblance of plateau regions near the beginning and end of the transient response. The picture is somewhat complicated because in this instance the amplitude response is dependent on time and a moving pulse leads to non symmetrical results because of aberration.

Of interest at this point is that the transient response, if viewed as the output of a non-uniform spatial array, can be improved by reducing the plateau. This can be accomplished by decreasing the frequency or the interval between elements. The constraint given by Eq. (3.20) allows any multiple of the fundamental frequency to be used

for focusing, yet any multiple of the fundamental will shorten the clean sweep region interval and raise the plateau region values.

For example, the same values used to generate figure 4-19(a) are again used except Δx is changed from 2 mm to 1 mm. This results in the transient response shown in figure 4-20. Note in this case the leading plateau region is nearly gone and the trailing plateau arrives substantially later in time. Also, note the mainlobe and associated sidelobes have increased in temporal extent as expected. The same results can be obtained by changing the center frequency to 1 MHz and leaving the interelement spacing at 2 mm.

The process of scanning and focusing is somewhat complicated and a similar example presented from another viewpoint may help explain the complicated transients.

The total pressure from an array system, as illustrated in figure 3-8, at a specified focal point (.1,.1) is due to a summation of pressures from each element in the array. The time required for the leading edge of a pulse to reach the focal point is presented in figure 4-16. The temporal extent of the contribution from each element is the pulse duration. Figure 4-21(a) illustrates the pressures arising from each element of a 60 element array with an interelement spacing of 2 mm. The center frequency of the LFM chirp is 1 MHz and focused at the line $y = .1$. Figure 4-21(b) is the result of summing the element contributions as a function of time.

At the time when the phase of all elements contributions is nearly the same, as indicated by the dashed line in figure 4-21, focusing occurs and a significant increase in the response is noted.

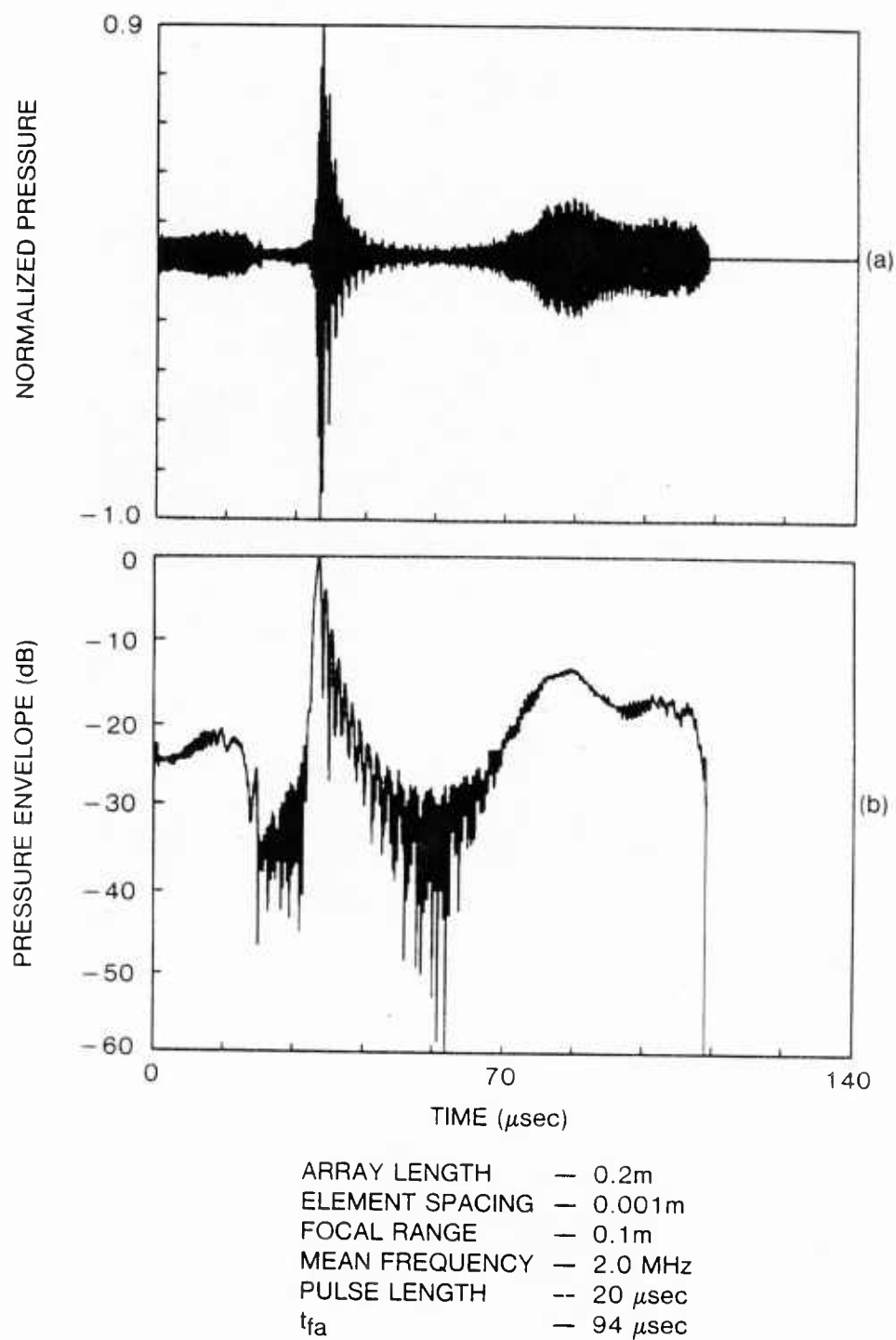


Figure 4-20. Transient Response with Interelement Spacing (1.3 mm).

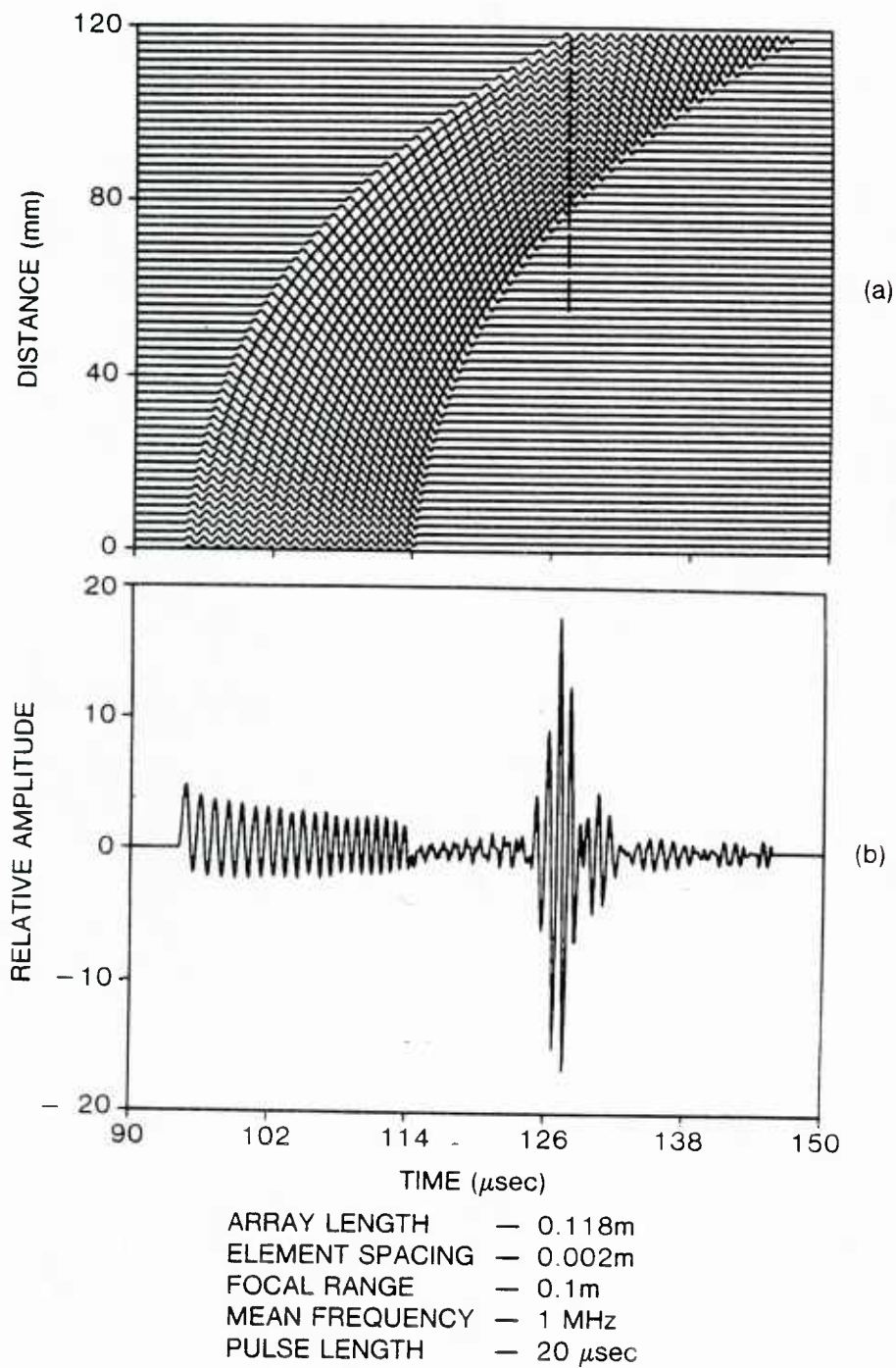


Figure 4-21. Signal Response from Individual Elements and Array at a Focal Point.

The previous results are based on an array of simple sources. Now consider the effects caused by transducers of finite length. As described earlier the result of this inclusion is to change the impulse response of a single element from a single positive pulse to a rectangular function. The duration and location in time is determined by the bearing of the spatial point of interest and the length of the radiator (see Chapter 3, section D). Selecting the same variables as used to produce figure 4-19(a) and including the effects of extended sources 1.3 mm in length leads to the results shown in figure 4-22. The principal effect is a reduction in amplitude of the plateau regions. A simple analysis of the beam response for a single element 1.3 mm in length driven at 2 MHz indicates a null in the beampattern at about 16 degrees. This indicates the most noticeable change in the transient response will occur relatively near the maximum response. If cancellation were desired at times corresponding to the center of the plateau region then somewhat shorter elements would be more appropriate.

Thus far the transient pressure response generated by a frequency focused and scanned line array has been investigated using the impulse response technique. The analysis is now extended to include a receiving array such that the transmit and receive response of an array can be evaluated.

Consider the case illustrated in figure 4-23 where an ideal reflector is located at a field point. Also assume, for simplicity it is only possible for energy radiated from the target to be received on the receiving array. The receiving array interelement spacing and radiator lengths are identical to those of the transmitter array. However, the receiving array is specified to have a conventional time

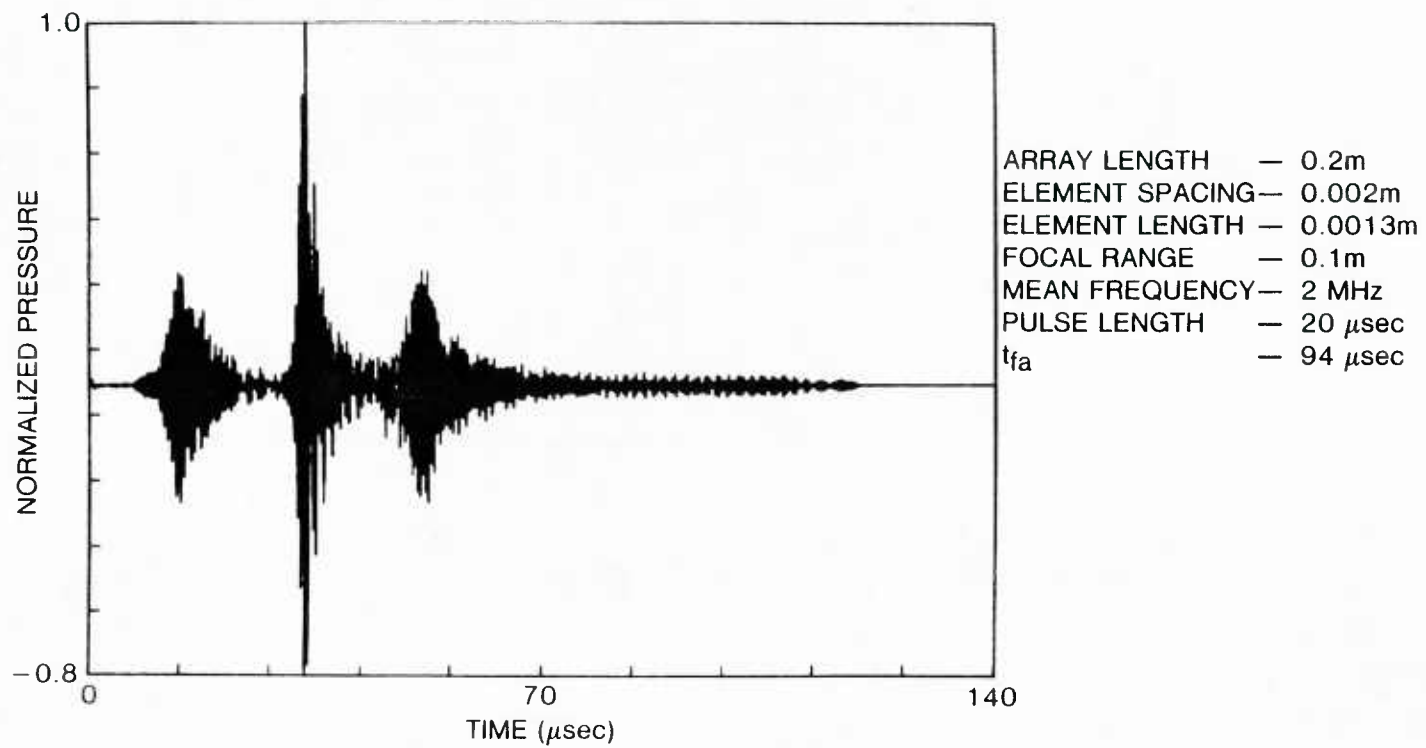


Figure 4-22. Transient Response from a Scanned and Focused Array of Extended Elements.

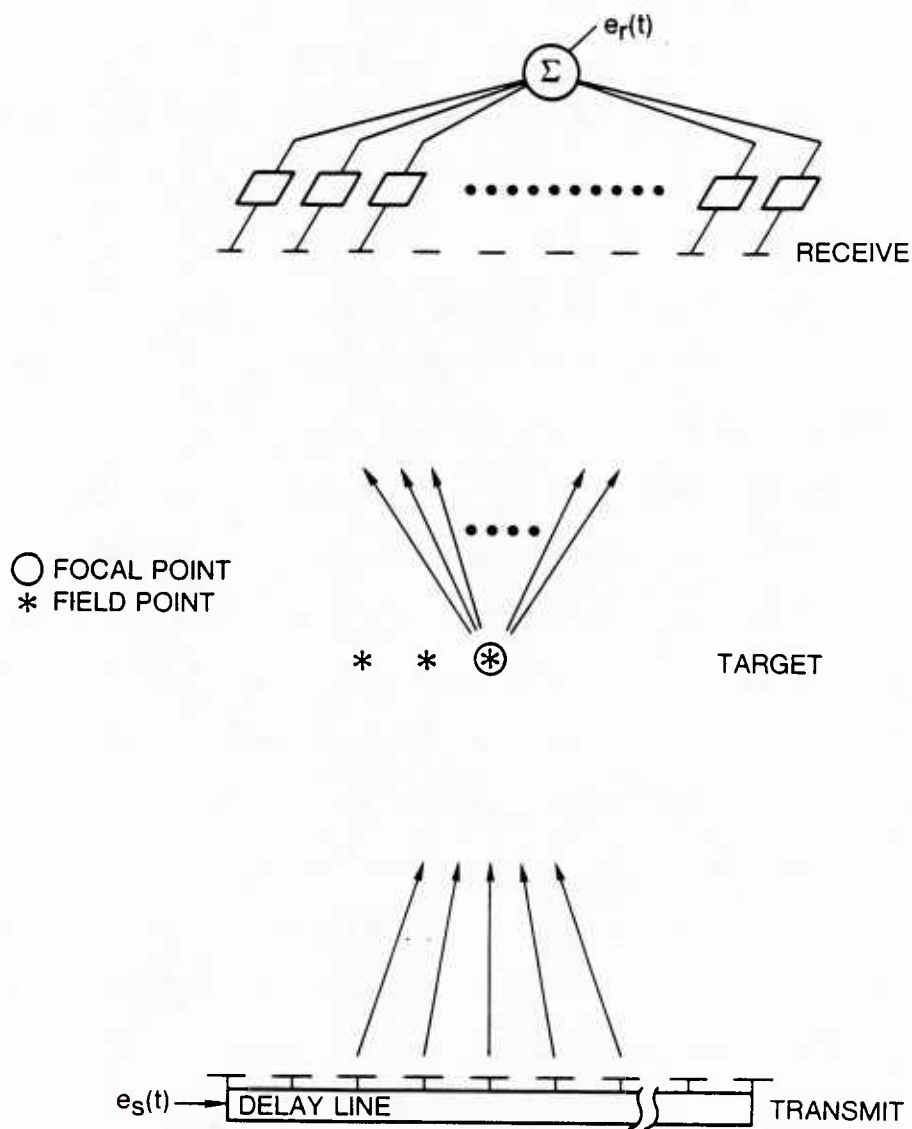


Figure 4-23. Conceptual Diagram of Frequency Focused and Scanned Transmitting Array and Time Delay Beamforming Receiving Array.

delay beamformer instead of a delay line for the purpose of focusing in the near field.

When the receive array is focused on the target located at $(.1,.1)$ the receive array system output is similar to the pressure radiated from the target as can be seen by comparing figure 4-22 and 4-24. This is as expected because there is no modification made by a time delay beamformer in the case of ideal focusing. The only change occurring is the result of the finite length radiators.

In the case when the receive beamformer is focused at spatial points other than the target location the beamformer and array elements will modify the receive array output. For example figure 4-25 a, b and c represent the transient response of the receive array system output when the transmit array is focused at $(.1,.1)$ and the receive array is focused at the three locations shown in figure 4-23 along the $y = .1$ line. Note the last position coincides with the target on the focal line of the transmitter system. It is easy to see the receive system is substantially affected by the focal point selected. What is not obvious because of the self-scaling graphs is the maximum values at the various points differ by almost a factor of ten between the values obtained at $x = .1$ and $x = .06$. Similar results are obtained whenever the receive system is not focused on the target.

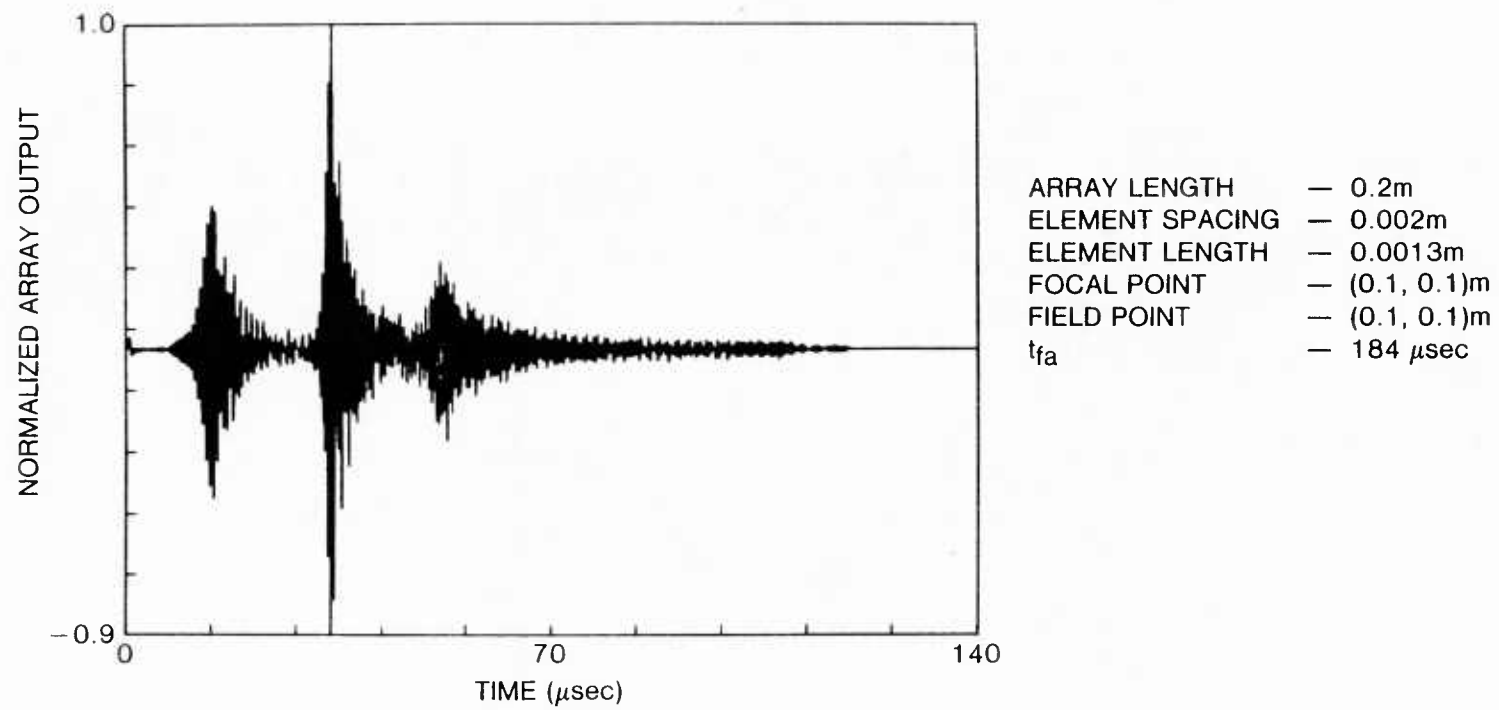


Figure 4-24. Transient Response of Receiving Array Focused on a Target.

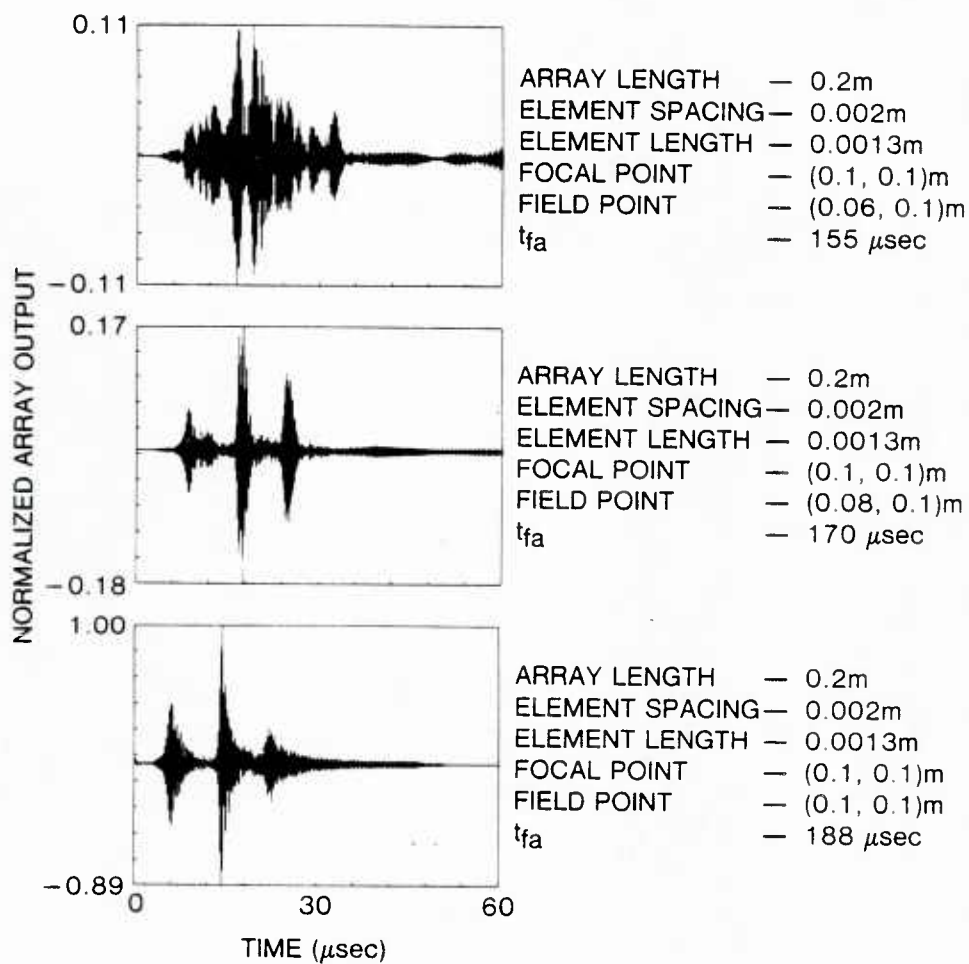


Figure 4-25. Transient Response of Receiving Array as Function of Receiver Beamformer.

V. SUMMARY AND CONCLUSIONS

An approach has been developed to analyze the transmit and receive transient pressure fields of line arrays with time delay beamformers. This approach is based on an extension of the spatial impulses response developed by Stepanishen for planar pistons in an infinite baffle. The impulse response function can be used to analyze array systems. The simple convolution of the spatial impulse response for an array system and an arbitrary source waveform can be used to analyze array system performance as a function of waveform design. This approach therefore can be used to conduct a rather complete systems analysis.

The impulse response for a curved or straight line array system is shown to be series of impulses when the elements can be treated as point sources. The magnitude of the impulses is determined by the geometrical properties of the array. Their locations in time are determined by the geometrical properties of the array and the beamformer time delays.

When the elements are of finite length and located far from the field point the impulse response for the element is a rectangular function. The duration of the rectangular function is related to element size and location relative to the field point.

In array systems of finite elements the single impulse of a point source is replaced with the appropriate rectangular function. The time interval between the pulses is then used to design waveforms for optimizing array system performance.

The spatial impulse response for a continuous line array with an internal propagation speed is developed as a linear superposition of

three dimensional point sources with initial excitation times dependent on their location within the array. The magnitude and duration of the spatial impulse response is dependent on the geometrical properties of the array, the speed of propagation within the array and media, and the location of the field point. In the far field this result reduces as expected to a rectangular function.

The impulse response for a complex array system of discrete elements and a delay line which can be used for scanning is developed. An analysis of the resultant impulse response is used to determine the type of signal waveform required to focus the output of the array. This waveform is then convolved with the impulse response to obtain the time dependent pressure field of this type of array at field points of interest.

Based on the numerical results obtained and favorable comparisons with other techniques when possible it appears the impulse response technique is a viable approach to analyzing the formidable problem of analyzing array systems subject to transient pressure fields. The technique yields a spatial impulse response which is dependent on the geometry of the problem and beamformer. The impulse response can then be convolved with a variety of signal waveforms to perform an array systems analysis as a function of waveform design.

Though not investigated there appear to be several areas where this technique may be modified or extended in a straightforward manner to examine other problems. In this thesis the input excitation waveform was modeled as if it were generated by a single function generator. There are no foreseen problems if the excitation at each element is independently controlled. This would permit the

introduction of amplitude and phase shading as well as frequency parameters in the array system analysis.

The arrays described in this study were considered to be line arrays; however, the technique can be extended to include planar or three-dimensional arrays without much difficulty.

In addition, it appears this approach can be used when the methods of source images are applicable. Thus, the impulse response technique may be used to analyze a much wider range of problems than considered at this time.

LITERATURE CITED

- Harris, G. R. "Review of Transient Field Theory for a Baffled Planar Piston." JASA vol. 70, no. 1. (July 1981): 10-20.
- Stepanishen, P. R. "Transient Analysis of Planar Sonar Arrays." Phd. Thesis, the Pennsylvania State University, Dec. 1969.
- Papoulis, A. Circuits and Systems - A Modern Approach. New York: Holt, Rinehart and Winston, Inc., 1980.
- Brigham, E. O. The Fast Fourier Transform. Englewood Cliffs, NJ: Prentice-Hall Inc., 1974.
- Morse, P. M.; and Ingard, K. U. Theoretical Acoustics. New York: McGraw-Hill, Inc., 1968.
- Steinberg, B. D. Principles of Aperture and Array System Design. New York: John Wiley and Sons, 1976.
- Stepanishen, P. R. "Pulsed Transmit/Receive Response of Ultrasonic Piezoelectric Transducers." JASA vol. 69, no. 6 (June 1981): 1815-1827.
- Stepanishen, P. R. "Transient Radiation from Pistons in an Infinite Planar Baffle." JASA vol. 49 no. 5 (part 2) (1971): 1629-1638.
- Proceedings of the IEEE. "Special Issue on Acoustic Imaging." IEEE vol. 67, No. 4 (April 1979): 452-664.
- Souquet, J.; Kino, G. S.; and Waugh, T. "Chirp Focused Transmitter Theory." Acoustical Holography vol. 6 (1975): 275-304.
- Applied Hydro - Acoustic Research, Inc. "Handbook of Array Design Technology - Volume I." Prepared for Naval Electronic Systems Command, 30 June 1976.

SELECTED BIBLIOGRAPHY

- Applied Hydro - Acoustic Research, Inc. "Handbook of Array Design Technology - Volume I." Prepared for Naval Electronic Systems Command, 30 June 1976.
- Bendat, J. S.; and Piersol, A. G. Random Data: Analysis and Measurement Procedures. New York: John Wiley and Sons, Inc., 1971.
- Brigham, E. O. The Fast Fourier Transform. Englewood Cliffs, NJ: Prentice-Hall Inc., 1974.
- Fraser, J.; Havlice, J.; et al. "An Electronically Focused Two-Dimensional Acoustic Imaging System." Acoustical Holography vol. 6 (1975): 275-304.
- Freedman, A. "Farfield of Pulsed Rectangular Acoustic Radiator." JASA vol. 49, no. 3 (part 2) (1971): 738-748.
- Hamming, R. W. Digital Filters. Englewood Cliffs, NJ: Prentice-Hall Inc., 1983.
- Harris, G. R. "Review of Transient Field Theory for a Baffled Planar Piston." JASA vol. 70, no. 1. (July 1981): 10-20.
- Harris, G. R. "Transient Field of a Baffled Planar Piston Having an Arbitrary Vibration Amplitude Distribution." JASA vol. 70, no. 1 (July 1981): 186-204.
- Havlice, J. F.; and Taenzer, J. C. "Medical Ultrasonic Imaging: An Overview of Principles and Instrumentation." IEEE Proceedings vol. 67, no. 4 (April 1979): 620-640.
- Kinsler, L. E.; Frey, A. R. Fundamentals of Acoustics. New York: John Wiley and Sons, 1962.
- Morse, P. M.; and Ingard, K. U. Theoretical Acoustics. New York: McGraw-Hill, Inc., 1968.
- Oppenheim, A. V.; Schafer, R. W. Digital Signal Processing. Englewood Cliffs, NJ: Prentice-Hall., 1975.
- Papoulis, A. Circuits and Systems - A Modern Approach. New York: Holt, Rinehart and Winston, Inc., 1980.
- Papoulis, A. Signal Analysis. New York: McGraw-Hill, Inc., 1977.
- Proceedings of the IEEE. "Special Issue on Acoustic Imaging." IEEE vol. 67, No. 4 (April 1979): 452-664.

SELECTED BIBLIOGRAPHY (cont.)

- Smith, J. M., "A Survey of Advanced Techniques for Acoustic Imaging." Army Materials and Mechanics Research Center, Watertown, MA. Rpt. No. AMMRC-MS-77-7 (Aug. 1977).
- Souquet, J.; Kino, G. S.; and Waugh, T. "Chirp Focused Transmitter Theory." Acoustical Holography vol. 6 (1975): 275-304.
- Stakgold, I. Boundary Value Problems of Mathematical Physics - Volume II. New York: The Macmillan Co., 1971.
- Steinberg, B. D. Principles of Aperture and Array System Design. New York: John Wiley and Sons, 1976.
- Stepanishen, P. R. "Acoustic Transients from Planar Axisymmetric Vibrators using the Impulse Response Approach." JASA vol. 70, no. 4. (Oct. 1981): 1176-1181.
- Stepanishen, P. R.; and Fisher, G. "Experimental Verification of the Impulse Response Method to Evaluate Transient Acoustic Fields." JASA vol. 69, no. 6 (June 1981): 1610-1617.
- Stepanishen, P. R. "Pulsed Transmit/Receive Response of Ultrasonic Piezoelectric Transducers." JASA vol. 69, no. 6 (June 1981): 1815-1827.
- Stepanishen, P. R. "Transient Radiation from Pistons in an Infinite Planar Baffle." JASA vol. 49 no. 5 (part 2) (1971): 1629-1638.
- Stepanishen, P. R. "Transient Analysis of Planar Sonar Arrays." Phd. Thesis, the Pennsylvania State University, Dec. 1969.
- Taylor, A. E. Advanced Calculus. Waltham, MA: Ginn and Co., 1955.
- Towne, D. H. Wave Phenomena. Reading, MA: Addison-Wesley Publishing Co., 1967.
- Young, J. W. "Electronically Scanned and Focused Receiving Array." Acoustical Holography vol. 7 (1977): 387-403.

INITIAL DISTRIBUTION LIST

Addressee	No. of Copies
COMOPTEVFOR	1
COMSURFWARDEVGRU	1
COMSUBDEVGRUONE	1
COMSUBDEVRON 12	1
ASN (RE&S)	1
OUSDR&E (Research & Advanced Technology)	2
Deputy USDR&E (Res & Adv Tech)	1
OASN, Spec Dep for Adv Concept	1
ONR, ONR-200, -400, -422, -425AC, -430	5
CNO, OP-03-EG, -090, -095, -098, -223	5
CNM, MAT-05, -03621, ASW-10, -13, -14	5
DIA, DT-2C	1
NRL	1
NRL, USRD	1
NRL, AESD	1
NORDA, Code 113, 200, 220, 240, 255, 260, 270	7
USOC, Code 241	1
USOC, Acoustic Environ Supp Detachment, Code 240	1
NAVOCEANO, Code 02, 6200	2
NAVELECSYSCOM, ELEX 03, 320, 417, -124	4
NAVSEASYSCOM, SEA-06B, -62, -36, -37A, -631X, -631Y, -92R	7
NAVAIRDEVCON	1
NOSC, J. W. Young, Code 830	2
NOSC, Code 6565 (Library)	1
NCSC, Code 724	1
NAVSURFWPNCEN, Code U31	1
NISC	1
NAVPGSCOL	1
NAVWARCOL	1
APL/UW, SEATTLE	1
ARL/PENN STATE, STATE COLLEGE	1
CENTER FOR NAVAL ANALYSES (ACQUISITION UNIT)	1
DTIC	1
DARPA	1
WOODS HOLE OCEANOGRAPHIC INSTITUTION	1
NATIONAL INSTITUTE OF HEALTH	1
ARL, UNIV OF TEXAS	1
MARINE PHYSICAL LAB, SCRIPPS	1
BBN (J. Heine)	1
ANALTECHNS	1
OPERRES INC. (Dr. V. P. Simmons)	1
GESY (D. Bates)	1
Biophysics Laboratory of the Dept. of Ophthalmology University of Nijmegen (W. A. Verhoef)	1
Bureau of Radiological Health (G. R. Harris)	1
University of Pennsylvania (B. D. Steinberg)	1
Stamford University (G. S. Kino)	1
Massachusetts Institute of Technology (P. M. Morse, K. U. Ingard)	2
University of Miami/RSMAS (H. de Ferrari)	1
University of Rhode Island (P. R. Stepanishen)	1

U213077

